Mitochondrial DNA as a sensitive surrogate to oxidative stress in prostate cancer cells and circulating lymphocytes

Sam Wai Chan

Division of Surgical Research
Department of Surgery
McGill University, Montreal
December 2009

A thesis submitted to McGill University in partial fulfilment of the requirements of the degree of M.Sc.

Abstract

Mitochondrial DNA as a sensitive surrogate to oxidative stress in prostate cancer cells and circulating lymphocytes

Sam Wai Chan

McGill University

Supervisor: Dr. Junjian Z. Chen

Co-supervisor: Dr. Simone Chevalier

Increasing evidence suggests that oxidative stress plays a causative role in prostate cancer initiation and progression. Furthermore, enhanced levels of systemic oxidative stress detected in lymphocytes are also associated with prostate cancer risk. Due to mtDNA's high sensitivity to oxidative stress, we hypothesize that mtDNA may serve as a surrogate to oxidative stress in cancer cells and lymphocytes. First, we improved the sensitivity of a novel method for mtDNA damage analysis and proposed a standardized protocol. Secondly, we developed an approach for quantifying systemic oxidative stress using mtDNA responses in circulating lymphocytes. Finally, we demonstrated differential mtDNA responses induced by oxidative stress in two isogenic prostate cancer cell lines with different metastatic potential. The more metastatic C4-2 was more susceptible to oxidative stress and prone to mtDNA damage and copy number change. These results offer new insights into prostate cancer progression.

Résumé

Génome mitochondrial, un marqueur sensible pour le stress oxydatif dans les cellules cancéreuses de la prostate et des lymphocytes

Sam Wai Chan
Université de McGill

Superviseur: Dr. Junjian Z. Chen
Co-superviseur: Dr. Simone Chevalier

De plus en plus d'études suggèrent que le stress oxydatif joue un rôle déterminant dans l'initiation et la progression du cancer de la prostate. Aussi, des niveaux élevés de stress oxydatif systémique mesurés dans les lymphocytes ont été associés à un risque accru du cancer de la prostate. Puisque le génome mitochondrial (ADNmt) est très sensible au stress oxydatif, nous postulons que ce dernier peut servir de marqueur pour le stress oxydatif dans les cellules cancéreuses ainsi que dans les lymphocytes. Dans un premier temps, nous avons accru la sensibilité d'une nouvelle méthode d'analyse du dommage de l'ADNmt. Ceci nous a permis de proposer un protocole de mesure standardisé. Deuxièmement, nous avons développé une méthode afin de quantifier le stress oxydatif systémique en utilisant les réponses de l'ADNmt des lymphocytes. Finalement, nous avons démontré que deux lignées cellulaires prostatiques isogéniques, LNCaP et C4-2, ayant un potentiel métastatique distinct, répondaient différemment au stress oxydatif induit expérimentalement. La lignée C4-2, à potentiel plus métastatique, était plus sensible au stress oxydatif, se traduisant par une plus grande susceptibilité de l'ADNmt à être endommagé. Ces résultats apportent donc une nouvelle avenue dans la compréhension de la progression du cancer de la prostate.

Table of Contents

List of Tables

List of Figures

List of Abbreviations

ADP	Adenosine diphosphate
ATP	Adenosine triphosphate
AZ	Anterior firbromuscular zone
BER	Base excision repair
bp	Base pair
BPH	Benign prostate hyperplasia
BRCA2	Breast cancer 2
CaCl2	Calcium chloride
CAPZB	Capping protein (actin filament) muscle Z-line, beta
CHEK2	CHK2 checkpoint homolog
CO2	Cytochrome oxidase 2
COI	Cytochrome c oxidase subunit I
CZ	Central zone
DHE	dihydroethidium
DMSO	dimethyl sulfoxide
DNA	Deoxyribonucleic acid
EDTA	Ethylenediaminetetraacetic acid
EPAC2	Exchange protein directly activated by cAMP 2
ETC	Electron transport chain
ETOH	Ethanol
FBS	Fetal Bovine Serum
GPx	Glutathione peroxidase
GSH	Glutathione
GSTP1	Glutathione S-transferase P
H_2O_2	hydrogen peroxide
HG PIN	High-grade prostatic intraepithelial neoplasia
HIF1α	Hypoxia inducible factor 1α
HO•	hydroxyl radicals
HPC1	Hereditary prostate cancer locus 1
Kb	Kilobase
Malondialdehyde	MDA
MgCl2	Magnesium chloride

MSR1	Macrophage scavenger receptor 1
mtDNA	Mitochondrial DNA
NAC	N-acetyl-l-cysteine
O2•-	superoxide
PBS	Phosphate-buffered saline
PBS-CMF	Phosphate-buffered saline calcium-magnesium-free
PCR	Polymerase chain reaction
PLL	Poly-L-lysine
PON1	Paraoxonase 1
Prx	Peroxiredoxin
PSA	Prostate specific antigen
PZ	Peripheral zone
REST	Relative expression software tool
RNASEL	Ribonuclease L
ROS	Reactive oxygen species
RPMI	acronym of Roswell Park Memorial Institute
rTth	recombinant Thermus thermophilus
SNP	single-nucleotide polymorphisms
SOD1	Superoxide dismutase 1
SOD2	Superoxide dismutase 2
TBARS	Thiobarbituric acid reactive substances assay
TZ	Transitional zone

1. Rationale and objectives

Increasing evidence suggests that enhanced levels of oxidative stress are associated with prostate malignancy. Cellular ROS not only promote cancer growth through signalling pathways, but also contribute to cancer initiation and progression through DNA damage and mutagenesis. As primary targets of oxidative stress in the cell, aberrations in mtDNA integrity and function may play an important role in the aetiology and progression of prostate cancer. Indeed, mtDNA damage and mutations are common in prostate cancer. A proteomic shift of cytochrome c oxidase subunits and altered metabolism in the mitochondria are associated with prostate cancer cells and tissues. We propose a mechanistic investigation on mtDNA responses to oxidative stress in prostate cancer cells with different metastatic potential may offer new insights into prostate cancer initiation and progression. Furthermore, we suggest that enhanced oxidative stress is not only an intrinsic characteristic of prostate cancer cells, but also a characteristic of the peripheral tissues of cancer patients that can be detected using mtDNA in circulating lymphocytes. Therefore, the detection of mtDNA as a surrogate of systemic oxidative stress may prove to be a non-invasive approach in studying prostate cancer risk and progression in epidemiological studies. The main objectives are:

(1) to develop a standardized step-by-step protocol for the analysis of mtDNA damage responses to oxidative stress using real-time PCR (Chapter 1); (2) to develop a new approach to measure systemic oxidative stress by quantifying mtDNA damage and stress responses in circulating lymphocytes (Chapter 2); and (3) to investigate differential mtDNA damage responses induced by oxidative stress in two isogenic prostate cancer cell lines with different metastatic potential (Chapter 3).

2. Introduction and Literary Review

2.1 Prostate

The prostate gland is an exocrine organ, part of the male urogenital system. The etymology of the word “prostate” comes from the Greek word “prostates” which literally means "one who stands before" or "protector". The main function of the prostate gland is to store and secrete prostatic fluids during ejaculation, usually in the first fraction of the ejaculate along with the majority of spermatozoa. This prostatic fluid, which makes up 30% of the ejaculate, is slightly alkaline [1] and contains proteins responsible for semen gelation, coagulation, liquefaction, and coating/uncoating of spermatozoa [2]. The alkaline nature of the prostatic fluids has the function of neutralizing the acidic vaginal tracks. Due to these factors, spermatozoa found in prostatic fluids have better motility, survival and protection of their DNA. Prostatic specific antigen (PSA) is one of the primary exocrine products secreted by the prostate. PSA is a 34 kDa glycoprotein responsible for the liquefaction of semen, which allows sperm motility [3]. This glycoprotein is expressed in the prostatic luminal epithelium and expelled in the semen during ejaculation; and under normal conditions, does not cross the basement membrane. However, in the occurrence of a benign prostate hyperplasia (BPH) or prostate cancer, it leaks out into the bloodstream. Conveniently, PSA in the blood can be used for prostate cancer screening [4].

2.2 Prostate Anatomy

A healthy normal human prostate is slightly larger than a chestnut. It is wrapped around the urethra just below the neck of the urinary bladder. The anatomy of the prostate is usually divided into four zones: peripheral zone (PZ), central zone (CZ), transitional zone (TZ) and anterior fibro-muscular zone [5]. The peripheral zone accounts for up to 70% of

a normal prostate in young men and it surrounds the distal urethra. Up to 68% of the prostate cancer originates from the peripheral zone, which is often associated to high-grade prostatic intraepithelial neoplasia (HG PIN) or dysplasia [5]. The central zone makes up 20% of the prostate gland and surrounds the ejaculatory ducts. It is responsible for roughly 8% of the cancer. The transitional zone surrounds the proximal urethra and composes 5% of the prostate. It is mostly responsible for BPH. The anterior fibro-muscular zone accounts for 5% of the prostate and is not associated to carcinoma since it does not contain epithelial cells. There exists another classification of the prostate anatomy in which the gland is separated into lobes: anterior lobe, posterior lobe, lateral lobe, and median lobe. The anterior, posterior and median lobes correspond roughly to the TZ, PZ and CZ, respectively. The lateral lobe spans across all four zones [5].

2.3 Prostate Cancer

In Canada, prostate cancer is the most common cancer in men and the third leading cause of cancer death for men [6]. For 2009, there has been an estimate of 25,500 new cases of prostate cancer and an estimate of 4,400 deaths resulting from the disease. In perspective, 129 in 100,000 men (age-standardized) are diagnosed with prostate cancer and 23 in 100,000 men (age-standardized) die from it [6]. Similar statistics are observed in the United States with age-standardized incidence and mortality rates of 159.3 per 100,000 men and 25.6 per 100,000 men, respectively [7]. In Canada, the incidence rate has been increasing gradually over the last twenty years. This can be attributed to the increased public awareness on prostate cancer and the advent of PSA as a convenient marker. Despite this increase in the incidence rate, a significant decrease in mortality rate has also been observed over the years. Early detection of prostate cancer by PSA and

digital rectal exams have allowed timely treatments at the early stages of prostate cancer, resulting in better prognostic outcomes. Despite the improvements, prostate cancer remains the leading cancer for men in Canada. Consequently, it is important to study its aetiology for better diagnosis and prognosis.

2.4 Risk Factors

Epidemiological studies have identified several risk factors for prostate cancer such as age, ethnicity, hereditary factors, diet, smoking and oxidative stress [8-10]. Old age is the most prevalent risk factor as incidence increase significantly after the age of 55, and almost two-thirds of the prostate cancer population are 65 and older [6]. Genetic predisposition from inheritance (about 5%) is also a high risk factor [11]. The hereditary prostate cancer locus-1 (HPC1) was the first locust identified [12-13], offering proof of a hereditary link to prostate cancer. Several other genes linked to family inheritance were discovered afterwards, such as EPAC2, RNASEL, MSR1, CHEK2, CAPZB, vitamin D receptor, PON1, and BRCA2 [13-17]. In addition, genetic predisposition can also stem from ethnic origins. A genetic variant on the chromosome 8q24.11 (microsatellite allele DG8S737), which is associated with prostate cancer, has been detected between the European and African populations [18]. This genetic variant occurs at a high frequency in African-Americans, and may be a contributing factor in the 50-60% higher incidence rate of African-Americans when compared to Americans from European descent [18]. Lifestyle and dietary habits are also important risk factors. It is well established that Japanese men have a lower incidence of prostate cancer than Caucasians from developed countries. Interestingly, the prostate cancer incidence rate in Japanese men from Hawaii is between Japanese's from Japan and Caucasians' in Hawaii [19]. Japanese men from

Japan generally consume a low-fat diet with a high content of soy products containing phyto-oestrogens, which have been shown to be protective against prostate cancer [20]. Moreover, it has been shown that a high-fat diet triggers higher production of reactive oxygen species (ROS) from cellular respiration, which are highly toxic to proteins, lipids and DNA in cells [21].

2.5 Oxidative Stress – General Overview

Oxidative stress is defined as a state of physiological imbalance between oxidant and antioxidant levels. ROS are most often found in the form of superoxide ($O_2^{\bullet -}$), hydrogen peroxide (H_2O_2), hydroxyl radicals ($HO^{\bullet}$), and nitric oxide (NO) in the body; the majority being generated as by-products in the mitochondria during cellular respiration [22]. Thus, oxidative stress is an unavoidable consequence of aerobic life. The level of reactivity of these ROS increases from superoxide to hydroxyl radicals. Depending on their nature and intracellular level, ROS have different effects on the body. It has been shown that low levels of ROS are able to promote cell proliferation through growth pathways, such as Ras-regulated signal pathways that are superoxide dependent [23]. On the other hand, high levels of ROS promote oxidative stress which damages DNA, proteins and lipids leading to mutations and cell toxicity [24-25].

2.6 Antioxidant Defence

Human cells have several levels of antioxidant defence against ROS [26]. The first line of defence includes superoxide dismutase 1 and 2 (SOD1 and SOD2), which reduce superoxide into hydrogen peroxide. Hydrogen peroxide can be further reduced to water by catalase or glutathione peroxidase (GPx), where the excess electron is passed on to

glutathione (GSH). The reduced form of GSH required by GPx exists in limited quantities in the cell, and therefore, needs to be replenished in order to maintain the reducing power of the antioxidant defence system. In addition, Peroxiredoxins (Prx) regulate cytokine-induced peroxide levels, mediating signal transductions in cells. Thioredoxins function as antioxidants by reducing various oxidized proteins such as ribonuclease, coagulation factors, and insulin [27]. As part of the second line of defence, enzymes such as catalase is responsible for reducing H_2O_2[27]. Moreover, there are repair mechanisms to remove DNA damage induced by oxidative stress, such as the base excision repair (BER) mechanism [28]. An imbalance between antixodiants and oxidants, either due to the shortcoming of one or more of these antioxidant defence mechanisms or an increase in ROS, may lead to oxidative toxicity and cancer risk.

2.7 Oxidative Stress in Lymphocytes

Blood is a body fluid whose main function is to deliver nutrients and oxygen to cells, as well as transport waste products away. Blood is composed of plasma, erythrocytes, leukocytes, and platelets. Erythrocytes account for 99% of the blood cells, while leukocytes make up the remaining 1%. Leukocytes can be further categorized into two main groups: polymorphonuclear cells which include neutrophils, eosinophils and basophils and mononuclear cells which include monocytes and lymphocytes [29]. Lymphocytes are often used to investigate systemic oxidative stress. Enhanced levels of oxidative stress detected in lymphocytes have been associated with diseases such as rheumatoid arthritis [30], neurodegenerative diseases [31-34], pulmonary disease [35], and cancers [36-41].

2.8 Oxidative Stress in Prostate Cancer

Increased oxidative stress appears to be a defining characteristic of many cancer cells. Low levels of ROS production in cancer cells may serve as mitogens to promote tumor growth [42-44]; as demonstrated by cellular ROS upregulating hypoxia inducible factor 1α (HIF1α) in the nucleus, leading to the activation of downstream genes involved in angiogenesis and tumor metastasis in prostate cancer [45]. Excessive levels of ROS can also induce DNA damage leading to tumour initiation and progression [46]. Many factors lead to the belief that the prostate may be especially vulnerable to oxidative stress. First, evidence has shown that there is a pro-oxidant shift in the metabolic activity of prostatic epithelial cells [47-48]. Secondly, DNA lesions induced by oxidative stress detected in prostate cancer are more than twice the amount than in normal tissues [49]. Furthermore, antioxidant defence mechanisms such as GPx, catalase, SOD1, and SOD2 appear to be defective in prostate cancer cells [50]. DNA strand break repair capacity involving Rad51 gene was also found to be defective in prostate cancer cells [51]. It was suggested that the combination of oxidative stress sustained from chronic inflammation and the inactivation of the glutathione S-transferase P (GSTP1) antioxidant defence gene may induce neoplastic transformation in normal epithelial cells, and interestingly, these neoplastic cells are even more sensitive to further oxidative stress [52-54].

2.9 Mitochondria and Mitochondrial DNA

The mitochondrion is a critical organelle in the cell that is responsible for energy production through cellular respiration. Its size ranges from 0.5 to 10 μm and its structure is composed of the outer membrane, the intermembrane space, the inner membrane, the cristae and the matrix. The mitochondrion produces energy in the form of

adenosine triphosphate (ATP) through oxidative phosphorylation. In addition to supplying energy, the mitochondrion is involved in signalling, cellular differentiation, control of cell cycles and cell growth, and apoptosis [21]. However, due to its oxidative phosphorylation activities, it is also the major source of endogenous ROS production in the cell [21]. Although the majority of the genes required for mitochondrial functions reside in the cell's nucleus, the mitochondrion has its own DNA stored in the matrix compartment. MtDNA is circular and haploid; it consists of 16,569 bp and exists in multiple copies in each cell. MtDNA has a unique structural feature, it exists as a mixture of supercoiled and relaxed conformations. The supercoiled form is functional and is required for replication and transcription, while the relaxed form is not functional and contains damage induced by single or double strand breaks. MtDNA contains a main regulatory region (the D-loop) and 37 genes encoding 13 polypeptides involved in the electron transport chain (ETC) [55-56]. Due to its close proximity to the ETC and lack of histone protection, mtDNA is prone to oxidative damage [57-60]. Moreover, unlike nuclear DNA repair processes, there is limited knowledge on mtDNA repair. Polymerase γ is the only polymerase present in mitochondria, so it is inevitably involved in mtDNA repair. BER is the main repair mechanism in the mitochondria, but surprisingly the mitochondria lacks nuclear excision repair which is responsible for the repair of bulky adducts [61]. Due to its vulnerability to oxidative damage, the mitochondrion and its mtDNA have been implicated in the aging process and several diseases, such as neurodegenerative disease, cardiac dysfunction, as well as cancer [21].

2.10 Mitochondria in Prostate Cancer

It has been recognized that cancer cells exhibit an altered energy metabolism: cancer cells depend greatly on aerobic glycolysis instead of mitochondrial respiration for obtaining ATP [62]. This was first observed by Warburg over 80 years ago when he detected a decrease in mitochondrial ATP formation and an increase in ROS production in cancer cells [42, 63-65]. This respiratory dysfunction in the mitochondria of cancer cells was later coined as the "Warburg effect". Recent proteomic studies have revealed a significant shift in down-regulation of mitochondrial cytochrome c oxidase (subunits I-III) compared to subunits (IV-VIII) from the nucleus during progression of prostate cancer from normal epithelium to invasive carcinoma [66]. Furthermore, this phenomenon has been linked with altered metabolism in prostate cancer [67]. Consistent with the mitochondrial dysfunction, frequent somatic mutations in mtDNA were identified in prostate cancer [68-72]. Moreover, mtDNA mutations identified in the cytochrome c oxidase subunit I (COI) were responsible not only for the complex IV defect, but also for the increased ROS production in the cybrid system and increased tumour growth in nude mice [71]. Thus, mtDNA mutation and dysfunction may play an important role in the aetiology of prostate cancer through increased ROS production. It is proposed that mitochondrion-generated ROS may diffuse into the nucleus as H_2O_2 where they would act as a nuclear DNA mutagen and cellular mitogen [21, 73].

Chapter 1

Measuring mtDNA damage using a supercoiling-sensitive qPCR approach

[74] Chan, S.W. and J.Z. Chen, Measuring mtDNA damage using a supercoiling-sensitive qPCR approach. Methods Mol Biol, 2009. 554: p. 183-97.

Connecting statement

Dr. Chen's lab previously developed a novel method for quantifying mtDNA damage, repair and total copy changes using real-time PCR, which has several advantages over existing methods such as gel electrophoresis and long PCR. In this chapter, we aim to improve the sensitivity of this novel method and to propose a standardized protocol for quantifying mtDNA damage responses not only in cell cultures, but also in clinical tissues. Chapter 1 of this thesis is a reproduction of our published work from a textbook [74]. The published work with the textbook formatting was included in the appendices.

Contributions

- MtDNA analysis on LNCaP cells performed by Jingson Chen
- Development of mtDNA analysis on snap-frozen tissues and fast real-time PCR *vs.* original real-time PCR experiments performed by Sam W. Chan
- Supervisor: Dr. Junjian Z. Chen

3.1 Abstract

Compromised mtDNA structural integrity can have functional consequences in mitochondrial gene expression and replication leading to metabolic and degenerative diseases, aging and cancer. Gel electrophoresis coupled with probe hybridization and long PCR are established methods for detecting mtDNA damage. However, each has its respective shortcomings: gel electrophoresis is at best semi-quantitative and long PCR does not offer information on the structure. To overcome these limitations, we have developed a new method with real-time PCR to accurately quantify the mtDNA structural damage/repair and copy number change. We previously showed that the different mtDNA structures (supercoiled, relaxed circular and linear) have profound influences on the outcome of the real-time PCR amplification. The supercoiled structure is inhibitory to PCR amplification, while relaxed structures are readily amplified. We will illustrate the use of this new method by quantifying the kinetics of mtDNA damage and repair in LNCaP prostate cancer cells induced by exogenous H_2O_2 treatments. The use of this new method on clinical samples for spontaneous mtDNA damage level will also be highlighted.

3.2. Introduction

Recent studies have shown that alterations in mtDNA can induce functional changes that play important roles in metabolic and degenerative diseases, aging and cancer [21]. The mitochondrion is responsible for energy production during cellular respiration, and the ETC lies at the center of this metabolic function. Situated in the inner membrane of the mitochondria, the ETC supplies energy to the cell through oxidative phosphorylation of adenosine diphosphate (ADP) to ATP. However, the ETC is also a major source of ROS [75-76]. Due to its close proximity to the ETC and lack of protecting histones, the mtDNA is susceptible to oxidative damage, which can potentially lead to changes in mitochondrial gene expression and to somatic mutations in many human cancers [64, 69, 77-79]. In the cells, mtDNA is composed of a mixture of supercoiled, relaxed circular and linear forms. The mature mtDNA has a supercoiled structure with an average of 100 negative super-helical turns [80]. This supercoiled conformation is susceptible to DNA strand breaks induced by oxidative damage, *i.e.*, a single strand break can lead to the disruption of the supercoiled structure. Since the supercoiled conformation is required for initiation of mtDNA replication and transcription [81-83], maintaining the integrity of the mtDNA structure is crucial to normal mitochondria function.

Several techniques have been developed to study mtDNA damage. Gel electrophoresis is frequently used to detect mtDNA conformational changes. However, this assay is not quantitative, and also involves a tedious coupling process of Southern blot and probe hybridization. While, long PCR allows the quantification of mtDNA damage, it provides little information on the mtDNA structure. To overcome these limitations, we developed a new approach using real-time PCR to quantify structural damage and copy number change of mtDNA. This method is based on several key findings [84] (a) Supercoiled

and relaxed DNA molecules have different efficiencies in PCR amplification. The supercoiled structure inhibits PCR amplification, while relaxed DNA is readily amplified (*see* Note 1). (b) Heat-treatment of DNA templates prior to real-time PCR can be used to artificially introduce strand breaks and relax mtDNA molecules, allowing quantification of the total amount of mtDNA copies. Thus, this new method is useful for quantifying not only structural damage, repair and copy number change of mtDNA in stressed cells in culture, but also the level of spontaneous damage of mtDNA in clinical samples. In this chapter, the new approach will be illustrated by studying mtDNA damage responses to acute oxidative stress in prostate cancer cells (LNCaP) treated by H_2O_2.

3.3. Materials and Instruments

3.3.1 Cell Collection for LNCaP (*see* Note 2)

1. PBS-CMF, phosphate buffered saline without $CaCl_2$, $MgCl_2$ (GIBCO, Invitrogen cat. No. 20012-027).
2. PBS-CMF/0.5 mM EDTA, to obtain 0.5 mM EDTA, add 500 µl 0.5M EDTA to 500 ml to PBS-CMF; 0.5 M EDTA pH8.0 (GIBCO, Invitrogen cat. No. 15575-020).
3. Trypsin/EDTA solution: 0.05% trypsin + 0.02% EDTA.
4. RPMI media 1640, with L-glutamine.
5. Fetal Bovine Serum (FBS).
6. Penicillin-Streptomycin (10,000 units/ml, 10,000 µg/ml respectively).
7. Complete RPMI medium: remove 50 ml RPMI from 500 ml bottle, add 50 ml FBS (to get 10% FBS) and 5 ml penicillin-streptomycin.
8. Poly-L-lysine (PLL) coated-dish (*see* Note 3).

3.3.2 DNA Extraction with Genomic-tip

3.3.2.1 Cell culture:

1- QIAGEN Blood & Cell Culture DNA Kit Mini. The kit contains the following: C1, G2, QBT, QC, QF buffers, protease, 25 genomic tips.

2- RNase A 2.5 ml (100 mg/ml).

3- Distilled water, DNAse and RNAse free.

4- 1x Tris/EDTA buffer solution (TE buffer): pH 8.0 ± 0.1, 10 mM Tris, and 1 mM EDTA.

5- Isopropanol (2-propanol) for molecular biology grade, minimum 99%.

6- 70% ethanol.

3.3.2.2 Snap-Frozen Tissue Samples:

1- Refer to material in **Section 3.3.1.** for cell culture with the following additional material.

2- Proteinase K (>600 mAU/ml).

3- Glass tissue grinder, ground glass Potter-Elvehjem type (Kontes).

4- Sterile surgical scalpel blades and handles.

3.3.3 DNA Quantification

3.3.3.1 Fluorometric Quantification of dsDNA Using PicoGreen®:

1- 96-well plate, black opaque, fluorometry compatible.

2- Quant-iT™ PicoGreen® dsDNA Assay Kit (Invitrogen, cat. No. P7589). The kit contains PicoGreen dye, 20x TE buffer, and lambda DNA standard (100 µg/ml).

3- Multi-well plate reader with fluorometric capabilities at excitation/emission wavelengths of 480nm/520nm respectively. (PerkinElmer 1420 Multilabel Counter Victor^{3}V).

3.3.3.2 Quantification by Nanodrop

1. Nanodrop spectrophotometer instrument.
2. Distilled water, DNAse and RNAse free.
3. 1X Tris/EDTA buffer solution (TE buffer): pH 8.0 ± 0.1, 10 mM Tris, and 1mM EDTA.

3.3.4 Template DNA Preparation and Heat Treatment

1- PCR machine: GeneAmp PCR system 9700 (Applied Biosystems).

2- 1X Tris/EDTA buffer solution, pH 8.0 ± 0.1, 10 mM Tris and 1 mM.

3.3.5 MtDNA Structural Damage and Repair Analysis using Real-Time PCR

3.3.5.1 Bio-Rad System

1- 2X IQ™ SYBR® Green Supermix 500x50 µl reactions (BIO-RAD cat. No. 170-8882).

2- 10 µM primer working solutions (primer sequences listed in Table 1).

3- Distilled water, DNAse and RNAse free.

4- $MgCl_2$ Solution, 50 mM. (BIO-RAD cat. No. 170-8872).

5- 96-well PCR plates, DNAse and RNase Free (BIO-RAD cat. No. 2239441).

6- Optical tape for plates (BIO-RAD cat. No. 2239444).

7- Real-time PCR detection system: MyIQ™ Single Color Real-Time PCR Detection System with iCycler™ thermocycler base (BIO-RAD).

3.3.5.2 Applied Biosystems (ABI) System

1- Power SYBR® Fast Green PCR MASTER MIX.

2- 10 μM primer working solutions (primer sequences listed in Table 1)

3- Distilled water, DNAse and RNAse free.

4- MicroAmp™ Fast Optical 96-well Reaction Plate with Barcode (0.1 ml).

5- Optical tape for plates (ABI).

6- Real-time PCR detection system: 7500 Fast Real-Time PCR System (ABI).

Table 1 Chapter 1 - Primer Sequences

Gene	Forward primer 5'-3'	Reverse primer 5'-3'
CO2 (mtDNA)	CCCCACATTAGGCTTAAAAACAGAT	TATACCCCCGGTCGTGTAGCGGT
D-loop (mtDNA)	TATCTTTTGGCGGTATGCACTTTTAACAGT	TGATGAGATTAGTAGTATGGGAGTGG
β-actin	TCACCCACACTGTGCCCATCTACGA	CAGCGGAACCGCTCATTGCCAATGG
β-globin	GTGCACCTGACTCCTGAGGAGA	CCTTGATACCAACCTGCCCAG

3.4 Methods

The supercoiled structure of mtDNA is sensitive to experimental artifacts and can be easily disrupted if not properly handled, thus it is important to always handle the cells and DNA samples with care. The following protocols are designed to minimize potential artificial DNA damage. This section will go through the logical workflow of the experiment from cell collection (Section 3.4.1) → DNA extraction (Section 3.4.2) of cells (Section 3.4.2.1) or frozen tissues (Section 3.4.2.2) → DNA quantification (Section 3.4.3)

→ DNA template preparation and dilution (Section 3.4.4) → real-time PCR analysis (Section 3.4.5).

LNCaP cells are used as an example for the cell collection protocol. A QIAGEN Blood & Cell Culture DNA Kit is recommended for DNA extraction, since this kit employs an ion-exchange system that does not oxidize purines during isolation, unlike phenol-based methods [85] (*see* Note 4). The QIAGEN recommended protocol has been modified (*see* Note 5) in order to recover both mtDNA and nuclear DNA. The protocol will also apply for frozen tissue preparation (*see* Note 6).

Following the DNA extraction, the concentrations of the DNA samples will be quantified. It is recommended (*see* Note 7) to perform two rounds of quantifications. The first round will measure the stock concentrations, and the second round, the precise concentration of 10 ng/µl working solutions prepared from the stock solutions. Two methods are recommended for this step: (Section 3.4.3.1) fluorometric quantification of dsDNA using PicoGreen®, and (Section 3.4.3.2) quantification by Nanodrop® spectrophotometer (*see* Note 8).

Prior to the real-time PCR analysis, half of the 1 ng/µl DNA template will be heat-treated while the other half will remain unmodified (original). The original and heated 1 ng/µl DNA templates will then be used for the detection of the mitochondrial markers (CO2 and/or D-loop) and a 5 ng/µl DNA template for nuclear gene markers (β-actin and β-globin). The method used for real-time PCR analysis is based on the relative quantification model suggested by Pfaffl [86].

3.4.1 Cell Collection (LNCaP)

Protocol for LNCaP cells

1. Remove RPMI medium from the dish by aspiration.
2. Gently add 5 ml PBS-CMF/EDTA, incubate for 1 min at room temperature
3. Remove the PBS-CMF/EDTA and add 2.5 ml of trypsin, incubate for 5 min at 37^{o}C.
4. Resuspend cells by adding 6 ml of RPMI medium to inactivate trypsin; gently mix up and down with pipetor aid to get rid of clumps.
5. Transfer cell suspension to a 15 ml tube, and put on ice.
6. Take a small aliquot of cell suspension for cell counting. (should be between 2 to 5 million cells)
7. Centrifuge at ~180 g for 6 min.
8. Remove medium and resuspend cells in 1 ml PBS-CMF. (If the cell suspension has more than 5 million cells, use 2 ml of PBS then split into two 1.5 ml tubes in Step 9)
9. Transfer to 1.5 ml tube, centrifuge at high speed for 2 min.
10. Remove supernatant, but leave enough to cover the cell pellet. Put on ice.
11. Store at -80^{o}C.

3.4.2 DNA Extraction with Genomic-tip For Cell Culture and Snap-Frozen Tissue

This is a modified protocol based on the QIAGEN protocol. Do not use the C1 buffer (*see* Note 5). Prewarm the QF buffer to 50^{o}C in a water bath. Cool the 70% ethanol to -20^{o}C.

3.4.2.1 For Cell Cultures

Prepare protease solution by adding 1.4 ml distilled water to the powdered protease. The recommended amount of cells for each preparation is 2 to 5 million.

1- Thaw cells on ice, resuspend cells by flicking the tube with fingers.

2- Add 1 ml G2 digestion buffer to tube. Immediately vortex at maximum speed for 25 sec (be consistent for all samples). Process one sample at a time and leave them at room temperature. Centrifuge briefly.

3- Add 3 µl RNase A to each sample. Invert to mix and centrifuge for several seconds.

4- Add 25 µl reconstituted protease. Invert to mix, but do not centrifuge afterwards. Incubate at 50°C for 1h in water bath. Continue on to step 5 in the next section "DNA Extraction with Genomic-tips".

3.4.2.2 For Snap-Frozen Tissue Samples

Proceed with one sample at a time. It is important to carry out the following steps as fast as possible since the tissue sample can degrade rapidly after thawing. Do not thaw the samples until needed for cutting or grinding (*see* Note 9). Homogenize the tissues manually; any motorized assistance will disrupt the mtDNA structure. It is recommended to carry step 1 to 3 on ice.

1- Prepare a mixture of 1.8 ml G2 buffer + 4µl RNAse A per sample, mix well.

2- Weigh tissue sample (around 10 mg to 50 mg) and cut into smaller piece if needed (*see* Note 10).

3- Add the tissue pieces and ~300 ul of the G2 buffer/RNAse A mixture into a glass tissue grinder to homogenize. Grind manually but do not over-grind as this will disrupt the mtDNA structure (*see* Note 11). Collect homogenate into a 2 ml tube.

Wash grinder with remaining G2 buffer/RNAse A solution and collect into the 2 ml tube.

4- Add 100 µl proteinase K (*see* Note 12). Invert to mix. Incubate at 50°C for 2 h. Repeat Steps 1-4 for the next sample. Then continue on to Step 5

DNA Extraction with Genomic-tips

5- Approximately 15 min before the end of the incubation in step 4, add 2 ml of QBT buffer to each genomic tip and let the buffer equilibrate the tips.

6- Take the samples out of the water bath, and vortex the digested samples for 10 s. at maximum speed. Then transfer each sample to a genomic-tip.

7- After the samples have flowed through the tip, wash the tip with 3 x 1 ml of QC buffer.

8- Elute the DNA into a 15 ml tube by adding 910 ul QF buffer (prewarmed to 50°C) twice into the genomic-tip.

9- Mix the eluted DNA by inverting the tubes and centrifuge at ~188 g. Aliquot solution equally into two 2 ml microcentrifuge tubes (~850 µl).

10- Precipitate the DNA by adding 700-800 µl of isopropanol to each tube. Mix by inverting and incubate for 10 min at room temperature (*see* Note 13). Centrifuge at 15,000-18,000 x g for 20 min at 4°C (*see* Note 14).

11- Remove and discard the supernatant, leaving the DNA pellet at the bottom of the tube. This pellet contains nuclear and mitochondrial DNA.

12- Wash the DNA pellet with 500 µl of 70% ethanol (ETOH) (-20°). Centrifuge at 15000 to 18000 g for 10 min at 4°C.

13- Remove and discard the supernatant. Repeat Step 12 once.

14- Remove the supernatant, three samples at a time, and let the DNA pellet dry to air for a brief moment. (*see* Note 15)

15- Dissolve DNA pellet with 80-200 µl of TE buffer. Aim for a final concentration of ~ 60 up to ~200 ng/µl.

16- Let the DNA samples sit at 4°C overnight to ensure that DNA is completely dissolved.

3.4.3 DNA Quantification (*see* Note 7)

3.4.3.1 Fluorometric Quantification of dsDNA Using PicoGreen®:

First Round of Quantification of the stock DNA Samples:

Initial quantification

1- Thaw the PicoGreen® dye in the dark at room temperature.

2- Mix DNA samples by gently flicking the tube. Centrifuge briefly.

3- Prepare the lambda DNA standard. The recommended 2X dilution series range from 20 to 0.625 ng/µl (6 standards).

4- Aliquot 99 µl of TE buffer and 1 µl of DNA sample into a single well. Repeat for duplicate well and proceed to next sample. It is recommended to first prepare a mix of 198 µl TE buffer and 2 µl DNA in a microcentrifuge tube and then aliquot 100 µl of the mixture into two wells.

5- Aliquot 90 µl TE buffer and 10 µl of the lambda standard into a well. Repeat for duplicate well and proceed to next lambda standard.

6- Prepare PicoGreen® solution: aliquot 5 µl of stock PicoGreen® into 0.995 ml TE buffer; 100 µl of this mixture is required for each well (keep in dark).

7- Aliquot 100 µl of PicoGreen® solution into each well, then mix by pipetting up and down.

8- Incubate in the dark at room temperature for 10 min.

9- Perform fluorometric measurement using a multiplate reader at excitation/emission lengths of 480 nm/520 nm.

10- Calculate the concentration of the stock DNA samples based on the standard curve.

11- Prepare a 10 ng/µl working solution from each DNA sample stock (volume: around 200 µl).

Second Round of Quantification of the 10 ng/µl DNA Samples:

Precise quantification

12- Repeat the steps from "First Round of Quantification". Aliquot 90 µl TE buffer and 10 µl 10 ng/µl of DNA sample into each well this time.

13- Measure the concentration of 10 ng/µl DNA working solutions. 1 and 5 ng/µl DNA templates will be prepared from each working solution.

3.4.3.2 Quantification by Nanodrop® (For model ND-1000) (*see* Note 8)

1. Choose the nucleic acid assay option from the Nanodrop software.
2. Initialize the machine with distilled water. Pipette 1 µl of water onto the reading pedestal. Click OK. After each reading, wipe off with clean tissue.
3. Make a blank reading with 1 µl TE buffer. Click Blank.
4. Place 1 µl of DNA sample and click measure.
5. Take triplicate measurements of each sample and use the average of the results.
6. Prepare 10 ng/µl working solutions from DNA samples stock. Quantify again to insure precise concentrations.

3.4.4 DNA Template Preparation and Heat Treatment

1- Prepare 5 ng/µl templates in TE buffer from the 10 ng/µl working solutions. (Volume: 200 µl)

2- Prepare 1 ng/µl templates in TE buffer from the 5 ng/µl templates. (Volume: 100 µl)

3- Aliquot 50 µl of 1 ng/µl DNA into a 0.2 ml PCR tube and proceed with the heat-treatment in step 4. The remaining half will serve as the original template.

4- Perform heat treatment on 50 µl of 1 ng/µl DNA by following this PCR protocol: 95^{o}C for 6 min and 10^{o}C for cool down.

5- 5 ng/µl DNA templates will be used for quantifying nuclear markers, and 1 ng/µl original and heated DNA templates will be used for mitochondrial markers.

6- Prepare a five-point standard using the stock DNA of the control sample. The recommended standard is a 5X dilution series ranging from 40 to 0.064 ng/µl. (*see* Note 16)

3.4.5 MtDNA Structural Damage and Repair Analysis using Real-Time PCR

To ensure optimal reproducibility, always prepare a master mix containing the SYBR Green Supermix and primers, and use aliquots of this mixture with the individual DNA samples. For example, LNCaP cells are treated with exogenous H_2O_2 to measure mtDNA damage during exposure and repair activity during recovery (Figure 1). The following protocol is performed in 30 µl reaction in triplicate using the Bio-Rad system.

1- Resuspend samples and standards gently by flicking. Centrifuge briefly.

2- Prepare and label 0.5 ml tubes for each sample and standard.

3- Prepare the total amount of master mix needed by adding the reagents in this specific order (Table 2), based on a six paired samples (*i.e.*, for six each original and heated 1 ng/µl DNA) and five standards.

Table 2 Real-time PCR recipe

Template points (triplicate, 30 µl/well)	Reactions	Reagents	1X	54X
5 DNA standards	15X	Distilled H_2O	10.8 µl	583.2 µl
6 Original 1 ng/µl DNA	18X	50 mM $MgCl_2$	0.6 µl	32.4 µl
6 Heated 1 ng/µl DNA	18X →	10 µM Forward primer	0.9 µl	48.6 µl
1 Blank	3X	10 µM Reverse primer	0.9 µl	48.6 µl
	54X	2X SYBR Mix (Bio-Rad)	15 µl	810 µl
			28.2 µl	1,522.8 µl

(*see* Note 17)

4- Aliquot 5.4 µl of DNA template into a 0.5 ml tube, add 84.6 µl of the master mix. Mix well by pipetting up and down. Put tube on ice until ready to load into wells.

5- Repeat Step 4 for each sample and standard.

6- Aliquot each template mixture into three wells (30 µl per well). Be careful to deposit the aliquot at the bottom of the well without creating bubbles. Avoid cross-contamination of the wells. Blank solutions without DNA will serve as negative controls.

7- Seal the plate with optical tape. If necessary, centrifuge the plate briefly to get rid of bubbles.

8- PCR program for mtDNA markers on the Bio-Rad system: cycle 1 (1X), 95.0°C for 1.5 min; cycle 2 (30X), step 1 at 95.0°C for 20 sec, step 2 at 61.0°C for 30 sec; cycle 3 (1X), 95.0°C for 1 min; cycle 4 (1X), 55.0°C for 1 min, cycle 5 (40X) 55.0°C for 10

sec with an increase of 1.0°C after each repeat for collecting melting curve data. Enable real-time data collection at cycle 2 step 2 (for ABI system, *see* Note 18).

9- At least one nuclear DNA marker is analyzed to serve as a reference gene for the analysis. To amplify the nuclear gene, calculate the amount of each reagent based on triplicates of five standards, six 5 ng/µl DNA samples, and one blank (36X). The PCR program is the same as in Step 8, except for 40X at cycle 2 (for ABI system, *see* Note 19).

10- The data can be analyzed with any relative expression software tool (REST) which is based on the Pfaffl formula:

$$R = \frac{\left(Efficiency_{\ target\ gene}\right)^{\Delta CP\,\text{target}\left(Mean\,Control - Mean\,sample\right)}}{\left(Efficiency_{\ reference\,gene}\right)^{\Delta CP\,ref\left(Mean\,Control - Mean\,sample\right)}} . \qquad \textbf{Equation 1}$$

Assign a nuclear gene as the reference gene and use the original 1 ng/µl from the control sample as the calibrator for analysis (Figure 2) (*see* Note 20).

3.5. Notes

1. The supercoiled structure inhibits the binding of oligonucleotide primers, preventing further amplification. In contrast, the relaxed forms (open circular and linear) allow effective primer binding and subsequent DNA polymerization. Thus, the relaxed forms of mtDNA are better substrates for PCR than supercoiled mtDNA.
2. Listed materials for culture of prostate cancer LNCaP cells. Substitute with appropriate reagents and buffers for cell lines to be used.
3. LNCaP cells detach easily in regular culture dishes. Prepare PLL coated dishes by adding 3 ml of 1% PLL solution to a 100 mm dish. Incubate for 5 min, then remove all solution from the dish. Dry in fume hood overnight.

4. There are other methods for DNA extraction such as Trizol; however, it has been shown that the Trizol procedure disrupts most structural features from the mtDNA (data not shown).
5. The C1 step removes cellular organelles including mitochondria during preparation, leading to loss of mtDNA.
6. Fresh snap-frozen tissue samples are suitable for structural analysis, but not paraffin-embedded tissues due to crosslinking.
7. The 2-step DNA quantification is optional but recommended, since it will limit the dynamic range of the samples during real-time PCR amplification, leading to reproducible quantification.
8. A conventional spectrophotometer can also be used for the two-step DNA quantification. We recommend using the Nanodrop spectrophotometer which requires only 1-2 µl of DNA sample for precise measurement.
9. It is not recommended to repeatedly freeze and thaw the same samples as this can degrade the quality of the DNA. If the tissue sample is to be used on separate occasions, cut the tissue into smaller pieces and make aliquot into separate tubes.
10. Work fast. It is not recommended to thaw the tissue sample until it is ready to be homogenized in the glass homogenizer. If the tissue sample is too hard to cut, thaw on wet ice.
11. After homogenization, there will still be residual pieces of tissue that are not completely homogenated. Do not continue grinding because this will disrupt the DNA structure. Instead, transfer everything to a 2 ml tube and proteinase K will digest the remaining pieces.
12. Proteinase K is used instead of the protease included in the kit because the former is more efficient in the digestion of the remaining tissue in the homogenate.

13. Unless the sample is exposed to harsh treatments during experiments, the precipitated DNA should look like long intertwined DNA fibers.
14. The DNA fiber is mostly nuclear DNA; mtDNA is too small to be seen in suspension. The high-speed centrifugation is needed to bring down the mtDNA and to form a pellet with nuclear DNA.
15. Do not over-dry the pellet since it will make it harder to dissolve in TE buffer.
16. A standard is needed to take into consideration PCR efficiency when using Pfaffl's relative quantification model. The standard is not required for the ΔΔCt method, but the efficiencies of different markers have to be optimized and validated.
17. It is recommended to add an additional 3-4 µl distilled water to the final mixture to compensate for the loss due to pipetting.
18. PCR program for mtDNA markers on the ABI system: cycle 1 (1X), 95.0°C for 30sec; cycle 2 (30X), step 1 at 95.0°C for 3sec, step 2 at 61.0°C for 30sec; cycle 3 (1X) add melt curve. Enable real-time data collection at cycle 2 step 2.
19. PCR program for nuclear DNA markers on the ABI system: cycle 1 (1X), 95.0°C for 30 sec; cycle 2 (40X), step 1 at 95.0°C for 3 sec, step 2 at 61.0°C for 30 sec; cycle 3 (1X) add melt curve. Enable real-time data collection at cycle 2 step 2.
20. There are various REST tools that are freely available on the internet: REST-XL, REST-MCS, and others.
21. Similar results were obtained with the analysis of the D-loop mitochondrial marker.
22. Similar results were observed with other cell lines, frozen tissues, and blood leukocyte samples. The Power SYBR® Fast Green PCR MASTER MIX from ABI and its 7500 Fast Real-Time PCR System platform made it possible to cut down the initial 95°C activation time to 30 sec (*see* Note 18). This should be taken into

consideration when analyzing clinical samples where small differences in spontaneous damage levels need to be measured.

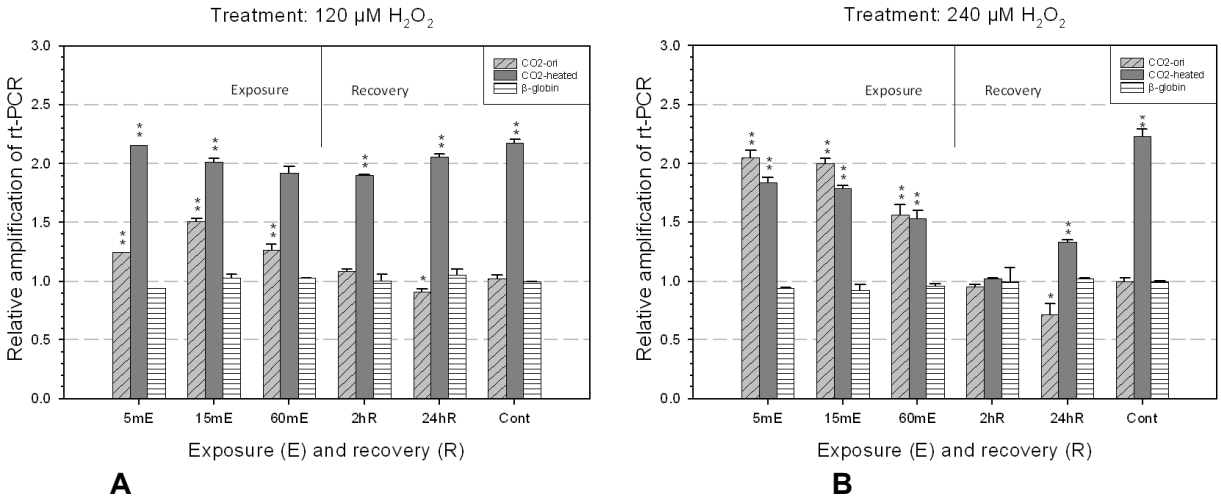

Figure 1 MtDNA damage responses to oxidative damage in LNCaP prostate cancer cells induced by exogenous H_2O_2 treatment.

Two concentrations (120 μM and 240 μM) of H_2O_2 were used to induce oxidative stress in LNCaP cells. For exposure, LNCaP cells were treated for 5, 15 and 60 min to induce DNA damage. For recovery, LNCaP cells were first treated for 60 min, and then allowed to recover in fresh medium for 2 and 24 h. The CO2 mitochondrial marker was normalized with the nuclear marker β-actin; a second nuclear marker, β-globin, was shown to indicate the lack of structural change in the target nuclear genes. The diagonally striped bars represent the relaxed mtDNA fraction in the original DNA template. The solid gray bars represent the total mtDNA content in the pre-heated mtDNA template. Changes in relaxed mtDNA fraction and total mtDNA content correspond to mtDNA damage and copy number change, respectively, in treated samples. (A) At low concentration of H_2O_2 (120 μM), LNCaP cells showed early increase of mtDNA structural damage from 5 minE to 60 minE when compared to control, but the damage was repaired 24 h after the treatment. The total mtDNA content remained stable. (B) While at a higher concentration of H_2O_2 (240 μM), LNCaP showed acute early mtDNA structural damage, reflecting complete disruption of mtDNA structure in the original template. The damage was not repaired 24 h after the treatment, resulting in a significant loss of mtDNA content as indicated by the decreases of total mtDNA signals in pre-heated templates. Statistics performed by one-way ANOVA with Dunnett's multiple comparison test, compared to original fraction of control (* = $p<0.05$, ** = $p<0.01$). (*see* Note 21)

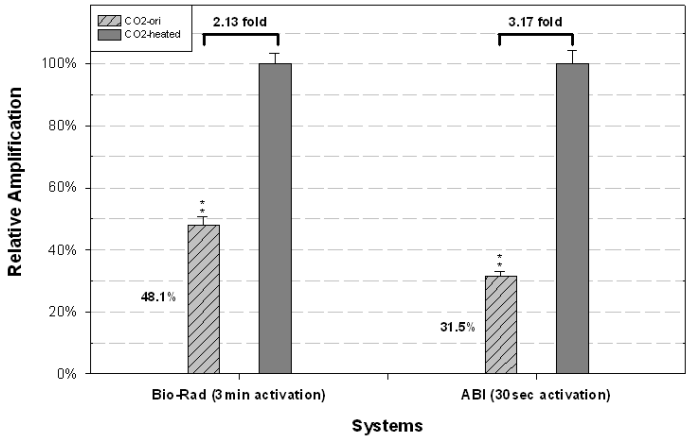

Figure 2 Baseline levels of mtDNA damage in non-treated prostate cancer cells analyzed by two qPCR systems: Bio-Rad vs ABI.

The baseline level of damage and the spontaneous damage are two distinct features. The baseline level of damage is the amount of mtDNA damage detected by the systems. Artifacts introduced during the sample preparation and the initial heat-activation of real-time PCR can increase the baseline level of damage. On the other hand, spontaneous damage represents the actual amount of endogenous mtDNA damage in non-treated samples. The mtDNA structure is heat sensitive, and consequently the initial enzyme activation step at 95^{o}C required by the real-time PCR protocol can potentially introduce artificial damage to the mtDNA structure. By shortening this step, it is possible to reduce this artificial damage. This figure compares the relative amplification of non-treated C4-2 (an isogenic variant of LNCaP) DNA using Bio-Rad and ABI systems at 3 min and 30 sec of initial 95^{o}C activation, respectively. The Bio-Rad system detected 48.1% of damaged mtDNA, while the ABI system detected 31.5% of damage. A reduction of 34.5% is observed between the two systems, representing the removal of substantial amount of artificial damage by the ABI system. As such, the baseline level of damage detected with the ABI system is more representative of the spontaneous level of mtDNA damage. The differences observed between the two systems can be attributed to the shorter initial heat-activation time as well as the different enzyme chemistry used. Statistics were performed with a t-test, the two groups were found significantly different (Bio-Rad (3 min), n=4; ABI (30 sec), n=3; ** = $p<0.01$) (*see* Note 22).

Chapter 2

Mitochondrial DNA as a sensitive surrogate to systemic oxidative stress

Authors: Chan, S.W., S. Chevalier, and J.Z. Chen

Manuscript in preparation

Connecting statement

Increasing evidence has shown that increased levels of systemic oxidative stress detected in circulating lymphocytes are associated with prostate cancer risk and progression, as well as various other pathologies, such as neuro-degenerative diseases, strokes, asthma, and obesity. But this thesis will mainly focus on prostate cancer. We suggest that enhanced levels of oxidative stress are not only a characteristic of prostate cancer cells, but also a characteristic of peripheral tissues of a cancer patient. In this chapter, we developed a new approach for the non-invasive detection of systemic oxidative stress using mtDNA damage in circulating lymphocytes.

Contribution

- All experiments performed by Sam W. Chan
- Supervisor: Dr. Junjian Z. Chen
- Co-supervisor: Dr. Simone Chevalier

4.1 Abstract

The general level of oxidative stress of the body, known as systemic oxidative stress, is associated with increased prostate cancer risks and progression. Also, increasing evidence has shown that oxidative stress in cancer cells is reflected in peripheral tissues such as lymphocytes. Consequently, it is important to have a sensitive and quantitative method for measuring systemic oxidative stress. MtDNA is a well studied marker for oxidative stress in cancer cells; thus, we propose that changes in mtDNA damage and content can be quantified in lymphocytes to serve as a non-invasive surrogate to systemic oxidative stress. Our goal is to develop a new approach using real-time PCR for measuring systemic oxidative stress by quantifying mtDNA content, endogenous damage and induced damage response. In the initial test, we compared the endogenous mtDNA damage and content between lymphocytes and two prostate cancer cell lines, C4-2 and LNCaP. Lymphocytes had significantly less endogenous mtDNA damage and content than the two prostate cancer cell lines. We further tested healthy lymphocyte samples by measuring the mtDNA damage response and repair after an exogenous H_2O_2 challenge. Up to 2.2-fold increase in mtDNA damage was detected when isolated lymphocytes were treated by 120 μM H_2O_2 for 15 min. In addition, no repair activity was observed after 1 hour of recovery. Similar mtDNA damage responses were observed with 1 ml of whole blood, suggesting that whole blood may serve as a convenient alternative to lymphocytes. Our new approach will help in the investigation of systemic oxidative stress, and may in turn lead to new findings in prostate cancer risk and progression research.

4.2 Introduction

Prostate cancer is the most prevalent cancer and the third leading cause of cancer death for men in Canada. Oxidative stress plays key roles in cancer initiation and progression [21, 76, 87-88]. Persistent oxidative stress induced by chronic inflammation has been associated with prostate cancer risk [89-91]. Enhanced susceptibility to oxidative injury due to a compromised antioxidant defence associated with ageing has also been linked to prostate cancer [91-92]. Moreover, ROS may induce molecular pathways leading to prostate tumorigenesis [45, 89, 93]. Thus, the enhanced level of endogenous oxidative stress found in prostate cancer and the tissue microenvironment may be actively involved in cancer initiation and progression.

Systemic oxidative stress may also be associated with carcinogenesis. For example, the reduced DNA damage repair capacity of lymphocytes caused by oxidative injury was associated with increased prostate cancer risk [36]. A direct correlation between DNA damage detected in lymphocytes and the level of DNA damage in prostate cancer tissues was observed in a study based on a dog model [37]. Moreover, increased susceptibility of serum lipids to peroxidation was linked to an aggressive form of prostate cancer [94]. Similar results were also observed in lung cancer [38], head and neck cancer [39], as well as other cancers [40] [41]. This data may suggest that enhanced oxidative stress is not only a property of the cancer cells, but also a general feature of a cancer patient's peripheral tissues. Systemic oxidative stress can be analyzed in blood cells using different methods. Host cell reactivation is a well established method for measuring DNA repair activity of lymphocytes [38, 95-96]; as is lipids peroxidation [97-99]. The comet assay is a widely used DNA-based method for determining oxidative damage as it measures nuclear DNA fragmentation. Damaged nuclear DNA strands diffuse outside

the lysed cell, where it forms a tail during single cell gel electrophoresis, hence the name comet assay. However, this method has limitations due to its semi-quantitative nature [100-101].

MtDNA is a sensitive marker to oxidative damage in cancer. Not only are changes in mitochondrial gene expression and mtDNA somatic mutations tightly associated with cancer cells [66, 69-70, 78, 84, 87-88, 102-104], but mtDNA abnormities have also been observed and associated with cancer patients' peripheral tissues. Xing *et al.* reported that lymphocytes from renal carcinoma patients contained significantly lower mtDNA content compared to a healthy population; postulating a correlation between low lymphocytic mtDNA content and increased risk of renal cell carcinoma [40]. In contrast Shen *et al*. observed a correlation between high mtDNA content in lymphocytes and increased breast cancer risk [105]. In addition, a correlation between high lymphocytic mtDNA deletions and increased risk of hepatocellular carcinoma was reported by Wu *et al.* [41]. However, differences in the quantity and integrity of circulating mtDNA in serum were not observed between prostate cancer patients and BPH patients [106]. The method of relative quantification with real-time PCR, as used in some of the above studies, has its limitations in population-based studies, due to extensive variation in mtDNA content between individuals [107]. Besides, the origin of the circulating mtDNA in serum is unknown in Ellinger *et al*.'s study [106]. Consequently, the nature of systemic stress is not clear. A better approach for quantitative analysis is needed to address some of the limitations.

In the current study, we proposed that mtDNA damage in lymphocytes can be used as a non-invasive marker of systemic stress. Our main goal was to develop a strategy for

measuring systemic oxidative stress by quantifying mtDNA damage and total content from circulating lymphocytes. Our objectives were: (1) to develop a simple approach for absolute quantification of mtDNA damage and content, (2) to evaluate the endogenous mtDNA damage and total content from lymphocyte samples, and (3) to quantify mtDNA responses to oxidative stress through H_2O_2 challenge. We also tested this new approach with whole blood samples as a convenient alternative to isolated lymphocytes.

4.3 Material and methods

4.3.1 Collection and preparation of prostate cancer cells, whole blood, and lymphocytes

LNCaP and C4-2 prostate cancer cells were cultured in RPMI media 1640 (GIBCO) with a supplement of 10% FBS (GIBCO) and 1% penicillin-streptomycin (GIBCO). LNCaP cells were cultured in 1% PLL (Sigma) coated dishes. The cells were collected with a Trypsin/EDTA solution, (0.05% trypsin + 0.02% EDTA, GIBCO), then washed down with PBS-CMF (GIBCO) and stored at -80^{o}C.

10 to 15 ml of blood was collected into blood collection tubes coated with EDTA (Fisher, Vacu 9ml K3EDTA PULL LAV). For experiments with whole blood, the samples were immediately stored at -80^{o}C in 10% dimethyl sulfoxide (DMSO) prior to treatment and analysis. For experiments with isolated lymphocytes, the lymphocytes were extracted from blood with Ficoll-Paque Plus (GE Healthcare) and were then stored at -80^{o}C in 40% RMPI media 1640 supplemented with 50% FBS and 10% DMSO solution prior to treatment and analysis. For the experiment with the absolute quantification of mtDNA content and damage (Figure 3), pre-isolated lymphocytes were supplied by Dr. Patrick

Walter from the Children's Hospital and Research Center in Oakland. All other lymphocyte and whole blood samples were obtained from healthy volunteers in our group.

4.3.2 H_2O_2 challenge experiment on lymphocytes and whole blood

Frozen lymphocytes were thawed at 37°C in a water bath for 1-2 min, and washed with 5 volumes of ice-cold wash medium to 1 volume of lymphocyte suspension (50% FBS and 50% RPMI 1640). The lymphocytes were counted and cell viability was assessed with trypan blue dye under microscope with an average of over 90%. A total of ~$3x10^6$ lymphocytes were incubated in 50 ml tubes with RPMI-1640 supplemented with 10% FBS for 30 minutes prior to the experiment. The lymphocytes were separated into three groups of ~$1x10^6$ cells each: untreated control, 120 μM H_2O_2 treatment for 15 min, and the same treatment with a recovery period of 60 min in fresh medium. The lymphocyte samples were washed with PBS-CMF, spun down to a pellet and then stored at -80°C before to DNA extraction and preparation.

Frozen whole blood was thawed at 37°C in a water bath for 1-2 min, and washed with 5 volumes of ice-cold wash medium to 1 volume of whole blood (50% FBS and 50% RPMI 1640). Whole blood cells were counted with trypan blue dye prior to incubation, and the average viability of white blood cells was over 90%. A total of ~$15x10^6$ white blood cells were incubated in RPMI-1640 supplemented with 10% FBS medium in 50 ml tubes for 30 min prior to the experiment. Whole blood samples were separated into three groups with ~$5x10^6$ cells each, similarly to the lymphocyte experiment. After the H_2O_2 treatment experiment, whole blood samples were collected and stored following the same protocol used on lymphocyte samples.

4.3.3 DNA preparation for structural-based real-time PCR analysis

DNA from prostate cancer cells, lymphocytes and blood cells were extracted with the QIAGEN Blood & Cell Culture DNA Kit according to its instructions with a few modifications to ensure that mtDNA and nuclear DNA were collected together [chapter 1 of this thesis]. Total DNA was quantified with a spectrophotometer (Nanodrop). DNA template solutions of 1 ng/µl were prepared for each sample with 1X Tris/EDTA Buffer Solution (pH 8.0, Fisher). Each template solution was split into two equal halves. Half of the solution was left unmodified as an original template and was used for the measurement of the relaxed mtDNA fraction [84]. The other half was pre-treated with heat at 95^{o}C for 6 min on a PCR machine and was used for the quantification of total amount of mtDNA [84].

4.3.4 Nuclear DNA and mtDNA standards preparation for absolute quantification

MtDNA standards were prepared for absolute quantification. A 3.3 kb mtDNA fragment containing the CO2 gene and a 2.5 kb fragment containing the D-loop gene were amplified from a human prostate cell line, RWPE-1, using the mtDNA primers listed in Table 3. The PCR was performed using the GeneAmp PCR system 9700 (ABI) with recombinant Thermus thermophilus (rTth) DNA polymerase (ABI). The three-step PCR amplification program was: pre-heat samples and add rTth polymerase once temperature reached 75^{o}C, 75^{o}C for 2 min, 94^{o}C for 1 min, 30 cycles of 94^{o}C for 15 sec, followed by 60^{o}C for 30 sec. and 72^{o}C for 3.5 min, then 72^{o}C for 5 min and cool down to 10^{o}C. Amplified DNA fragments were purified with the Qiagen PCR Purification Kit (Qiagen) and quantified for precise copy number according to the following equation from Figure 4:

$$copies\ /\ \mu l = \frac{[ng\ /\mu l]}{m}$$ **Equation 2**

Six serial dilutions were made from $3x10^6$ to 30 copies with a dilution a factor of 10X.

The nuclear DNA standards were prepared with a similar procedure. The nuclear primer sequences are listed in Table 3. A 2.7 kb nuclear fragment containing the Calicin gene was amplified from RWPE-1. Calicin is a single-copy nuclear gene which encodes for a basic protein of the sperm head cytoskeleton, and it exists in all cell types. Six serial dilutions were made from $3x10^6$ to 30 copies with a dilution factor of 10X.

4.3.5 Quantification of MtDNA damage and content using real-time PCR

The mtDNA damage analysis and total content were quantified by real-time PCR. The amount of damaged mtDNA and total mtDNA content were measured by quantifying the original DNA templates and pre-heated DNA templates respectively. The original templates were used for the nuclear DNA marker Calicin. In this study, the Applied Biosystems (ABI) 7500 Fast Real-Time PCR System with Power SYBR® Fast Green PCR MASTER MIX (ABI) was used for the analysis [74][Chapter 1 of thesis]. The original DNA templates, pre-heated DNA templates and standards were analyzed in triplicate in the same plate every time. The two-step PCR amplification program for both nuclear DNA and mtDNA was: 95.0°C for 30sec, 40 cycles of 95.0°C for 3 sec followed by 60.0°C for 30 sec. A melt curve analysis was enabled at the end of amplification. The primer sequences are listed in Table 3. The copy numbers of CO2, D-loop and Calicin were calculated based on the standard curve. For Calicin, since it is a single copy nuclear gene, the cell number could be calculated with the following equation from Figure 4:

$$\boldsymbol{Cell\ \#} = \frac{\textbf{Calicin copy number}}{\textbf{ploidy of cell}}$$ **Equation 3**

The exact copies of damaged and total mtDNA per cell were calculated from:

$$mtDNA\ copies/cell = \frac{\text{CO2 or D-Loop copy number}}{\text{cell \#}} \qquad \textbf{Equation 4}$$

4.3.6 Data analysis

All statistical analyses were performed with the aid of Graphpad Prism version 4 software. Unless specified otherwise, the data was analyzed with one-way ANOVA.

Table 3 Chapter 2 - Primer Sequences

Primers	Forward 5'-3'	Reverse 5'-3'
CO2 3285 bp long fragment	CCTAGGGTTTATCGTGTGAG	CTAGTTAATTGGAAGTTAACGG
D-loop 2467 bp long fragment	CGCACGGACTACAACCACGAC	CTGTGGGGGGTGTCTTTGGGG
Calicin 2658 bp long fragment	ATTCCAGAAGCCTTTAACTAG	ACAAATGAGACACAAACTACCG
CO2 (for real-time PCR)	CCCCACATTAGGCTTAAAAACAGAT	TATACCCCCGGTCGTGTAGCGGT
D-loop (for real-time PCR)	TATCTTTTGGCGGTATGCACTTTTAACAGT	TGATGAGATTAGTAGTATGGGAGTGG
Calicin (for real-time PCR)	CTGGTCGCTACATCTACATCTC	CAGGTCAGGCAACTTGGTC

4.4 Results

4.4.1 Approach for absolute quantification of total and damaged mtDNA

We have devised a new approach for the absolute quantification of the mtDNA structural damage and total copy number. The newly improved protocol, illustrated in Figure 3, is comprised of four main steps. The first step consisted of the construction of mtDNA and nuclear DNA standards (Figure 3A). 2 to 3 kb DNA fragments containing CO2 and D-loop mtDNA genes, as well as Calicin nuclear gene, were amplified by PCR from a human prostate cell line. The concentration (copies/µl) of these long DNA fragments were quantified and calculated according to the equation: "copies/µl = [ng/µl] / m". 10X serial dilutions were then produced to create the mtDNA and nuclear DNA standards. The second step was to prepare DNA templates for real-time PCR analysis (Figure 3B). Each DNA template was split into two equal halves. One half was left unmodified, which was used for the quantification of relaxed mtDNA and Calicin nuclear DNA copies. The other half was pre-treated to heat at 95^{o}C for 6 min, and was used for quantifying total mtDNA. The third step consisted of the real-time PCR absolute quantification analysis (Figure 3C). The results were expressed as mtDNA copies/cell. To do so, the exact amount of mtDNA and nuclear DNA copies were quantified and calculated from the standard curves according to the equation: copies = "10(CT-b)/a". The cell number was derived from "cell # = Calicin copies / ploidy of cell". The final step was the interpretation of the data (Figure 3D). With this approach, the amount of damaged mtDNA copies/cell, total mtDNA copies/cell, and endogenous mtDNA damage were quantified simultaneously. The endogenous damage was calculated from the ratio of damaged mtDNA/total mtDNA.

4.4.2 Absolute quantification of total mtDNA and endogenous mtDNA damage in lymphocytes and prostate cancer cells

Lymphocyte samples and two isogenic prostate cancer cell lines, C4-2 and LNCaP, were analyzed for the absolute copy number/cell for the mtDNA content and damage. In lymphocytes, the total mtDNA content was quantified at 153.25 ± 21.02 copies/cell and the amount of damaged mtDNA was 41.44 ± 7.87 copies/cell. This represented 27.04% of endogenous damage (Figure 4), calculated as the ratio of damaged mtDNA/total mtDNA. In comparison, prostate cancer cells, C4-2 and LNCaP, had a much higher mtDNA content of 990.41 ± 6.77 (*vs.* lymphocytes, $p<0.01$) and 3086.61 ± 48.27 (*vs.* lymphocytes, $p<0.01$) copies/cell, respectively. The levels of endogenous damage detected from the prostate cancer cell lines were 31.19% and 32.09%, respectively, which were significantly higher than that of lymphocytes ($p<0.05$). Thus, we were able to obtain absolute quantities on mtDNA total content, damaged molecules and endogenous damage of lymphocytes.

4.4.3 MtDNA damage response induced by exogenous H_2O_2 challenge in lymphocytes

To evaluate mtDNA damage responses, lymphocyte samples were treated with exogenous H_2O_2. Isolated lymphocytes for each healthy volunteer were separated into three groups: untreated control, 120 μM H_2O_2 treatment for 15 min, and 120 μM H_2O_2 treatment for 15 min followed by 60 min of recovery. The averages of total mtDNA content and endogenous mtDNA damage of the untreated control samples were 141.48 ± 14.22 copies/cell and 26.68%, respectively (Figure 5A). For H_2O_2 treated samples. the induced damage increased significantly from 26.68% to 59.28% ($p<0.01$), which represented a 122.19% increase in damage from the control. In addition, the damage was

not repaired after 60 min of recovery, suggesting that there was an absence of repair capacity during the recovery period. However, the total mtDNA content was not affected by the H_2O_2 treatment, and remained stable across all groups.

4.4.4 MtDNA damage response induced by exogenous H_2O_2 challenge in whole blood

As an alternative to lymphocytes, whole blood was tested using the same treatment performed on lymphocytes. The average endogenous mtDNA damage of the untreated control sample was 26.63%, similar to lymphocytes (Figure 5B); the total mtDNA content was 109.44 ± 22.40 copies/cell. After H_2O_2 treatment, induced damage was observed, the damage increased significantly from 26.63% to 36.74% ($p<0.05$), representing a 37.96% increase in damage. Similarly to lymphocytes, there was an absence of repair activity within 60 min after the H_2O_2 treatment, and the total mtDNA content was not affected. Although the mtDNA damage responses from whole blood samples were not as pronounced as the ones observed in isolated lymphocytes, the overall response pattern was very similar. Both sample types started with a relatively low endogenous damage level, followed by a significant increase in induced damage and a lack of mtDNA repair activity after recovery period. This suggested that lymphocytes and whole blood behaved similarly under exogenous H_2O_2 challenge.

4.5 Discussion

We have developed a new approach for analyzing systemic oxidative stress by quantifying mtDNA damage and total copy number in lymphocytes. The devised protocol covered three main steps: a) nuclear DNA and mtDNA standard preparation, b) DNA sample preparation, and c) real-time PCR analysis of mtDNA damage and total copy

number. With this new approach, we demonstrated that the lymphocyte samples had significantly less total mtDNA copies/cell and endogenous mtDNA damage when compared to both prostate cancer cell lines. Although mtDNA copy numbers in lymphocytes have been reported previously [108], damaged mtDNA copies/cell and endogenous mtDNA damage were reported for the first time in this study. When lymphocytes were challenged by H_2O_2, rapid mtDNA damage was induced, and not repaired. We also demonstrated that whole blood, after treatment of H_2O_2, had a similar response as isolated lymphocytes, suggesting a convenient alternative for mtDNA damage analysis. In short, the new approach developed in this study has the flexibility for non-invasive investigation of systemic oxidative stress through quantification of absolute copy numbers, endogenous damage levels and induced stress responses.

Our new and non-invasive approach represents a valuable alternative for measuring systemic oxidative stress since it has several advantages over existing methods. First, it is a sensitive method for quantifying mtDNA damage and total copy number, expressing results in absolute quantities of mtDNA copies/cell. Relative quantification of mtDNA with real-time PCR [40, 105] may be a convenient assay but, unlike our approach, the results are expressed as relative quantities normalized to an untreated control sample. Due to variations in mtDNA content between individuals [107], this reliance on the normalization of a control sample becomes a limitation. Consequently, the reference point is relative and changes from study to study. It effectively becomes a difficulty to compare different data sets. More importantly, the implications of supercoiled mtDNA [109] were not explicitly taken into consideration during real-time PCR amplification. Therefore, there is a high likelihood that only a fraction of mtDNA was quantified instead of total mtDNA content. Secondly, our approach measures mtDNA in lymphocytes

which has been a widely used marker in studies to reflect the systemic oxidative stress of an organism. In contrast, the implications of assays based on free floating mtDNA in serum are not well understood in the context of systemic oxidative stress. The origin of this floating mtDNA has not been well studied and documented, thus the nature of systemic oxidative stress is not clear. Additionally, because our approach is cell-based, it is possible to measure the oxidative stress response from lymphocytes. This oxidative stress response cannot be elicited with free floating mtDNA. Thirdly, we have devised a reliable and reproducible protocol for quantifying mtDNA over a large dynamic range from 30 to 3.0 x 10^6 copies. One of the most widely used assays for systemic oxidative stress analysis is the comet assay [36-37]. However, it is a semi-quantitative assay that relies on the visual grading of scorers [101]. Additionally, saturation occurs when most of the DNA is in the tail, and, as a result, the assay has a limited dynamic range. This may cause problems for measuring samples with high damage levels [101]. Detection of lipid peroxidation through malondialdehyde (MDA) with thiobarbituric acid reactive substances assay (TBARS) is one of the most widely method used for assaying oxidative stress due to its ease of use. But TBARS has been criticized of not being a specific marker of oxidative stress [110]. Taken together, our approach may be an alternative that researchers can use for analyzing systemic oxidative stress.

Our approach for measuring systemic oxidative stress may contribute to prostate cancer research. First, high levels of systemic oxidative stress have been associated with increased prostate cancer risk [36-37]. Our approach may allow researchers to assess prostate cancer risk in the general population in epidemiological studies. To test this hypothesis, a case-control study of age-matched healthy males *vs.* prostate cancer patients can be conducted. Secondly, elevated systemic oxidative stress has also been associated

with aggressive forms of prostate cancers [94]. Our approach may be used to assess prostate cancer progression. This can be used to screen for the more aggressive prostate cancers in patients, supplying additional data to physicians for a better judgment on prognosis outcome.

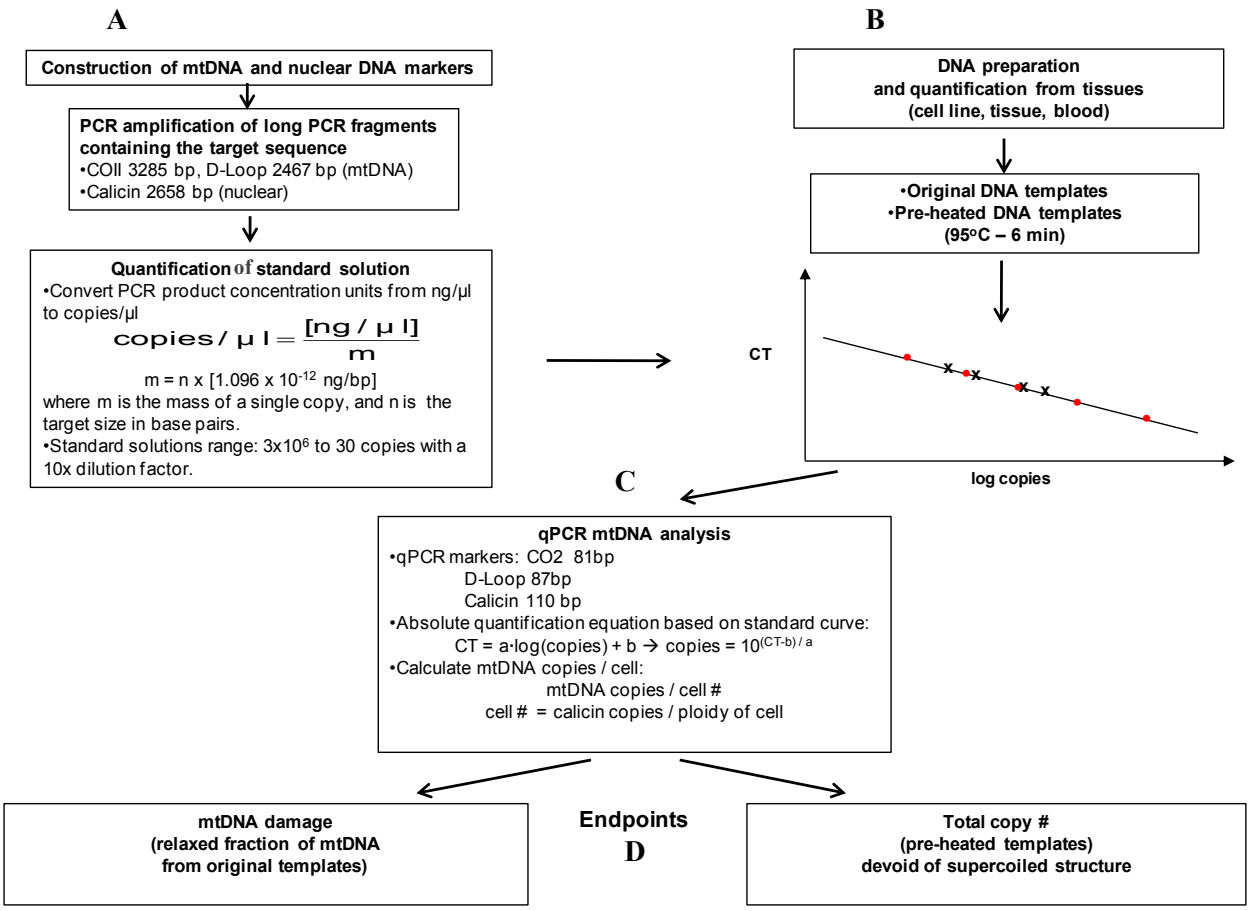

Figure 3 Approach for absolute quantification of total and damaged mtDNA.

This protocol is separated into four main steps. The first step (A) consisted of constructing the mtDNA and nuclear DNA standards. Long fragments of genes which contained the shorter real-time PCR targets were amplified and a 10X serial dilution was made from $3x10^6$ to 30 copies. In the second step (B), the original and pre-heated DNA templates were prepared from lymphocytes DNA samples and were used in the analysis for quantifying damage and total mtDNA, respectively. The third step (C) consisted of the real-time PCR absolute quantification analysis of mtDNA damage and total content. The fourth step (D) was the interpretation of the data.

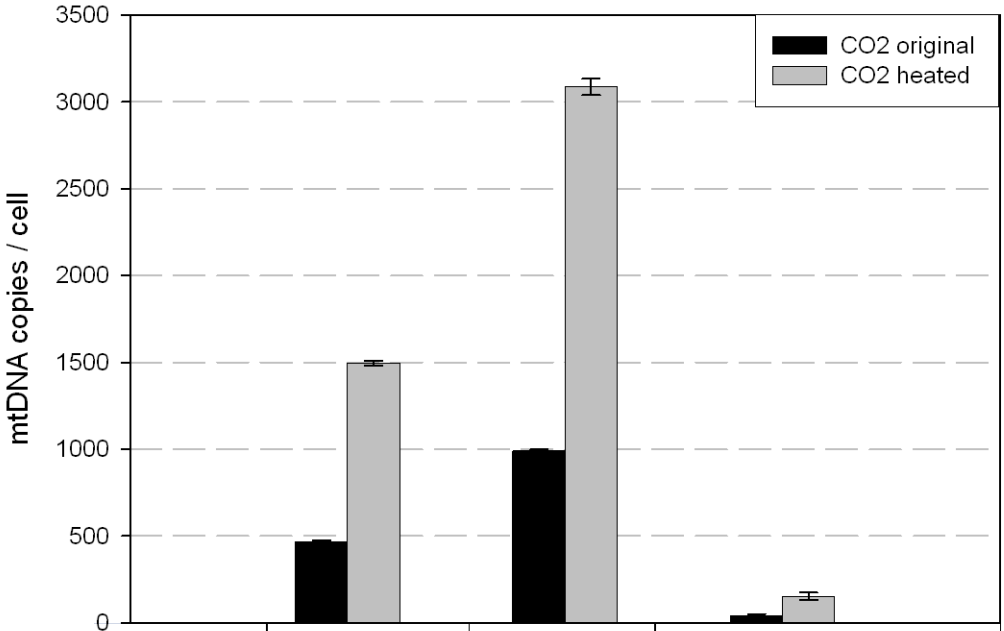

	C4-2	LNCaP	Lymphocyte
CO2 original	466.44	990.41	41.44
CO2 heated	1495.35	3086.61	153.25
% damage	31.19	32.09	27.04

Figure 4 Absolute quantification of total mtDNA and endogenous mtDNA damage in lymphocytes and prostate cancer cells.

C4-2 (n=2), LNCaP (n=2), and lymphocytes (n=4) were analyzed by real-time PCR for total mtDNA content, damaged mtDNA number, and level of endogenous damage. The cell number was calculated from Calicin copy numbers, a single copy nuclear marker. With mtDNA CO2 marker, the original (CO2 original) and pre-heated (CO2-heated) DNA templates were quantified for damaged mtDNA number and total mtDNA content, respectively.

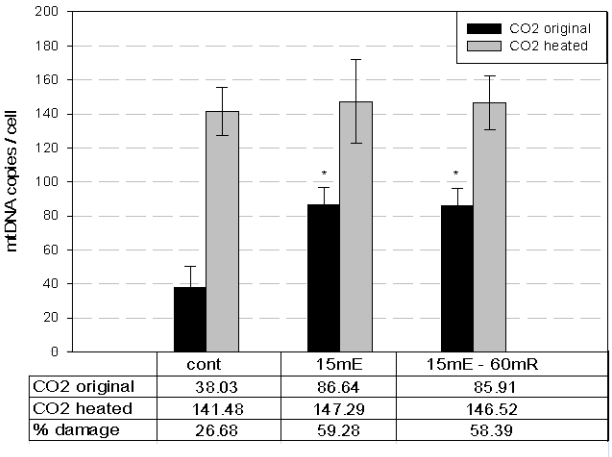

	cont	15mE	15mE - 60mR
CO2 original	38.03	86.64	85.91
CO2 heated	141.48	147.29	146.52
% damage	26.68	59.28	58.39

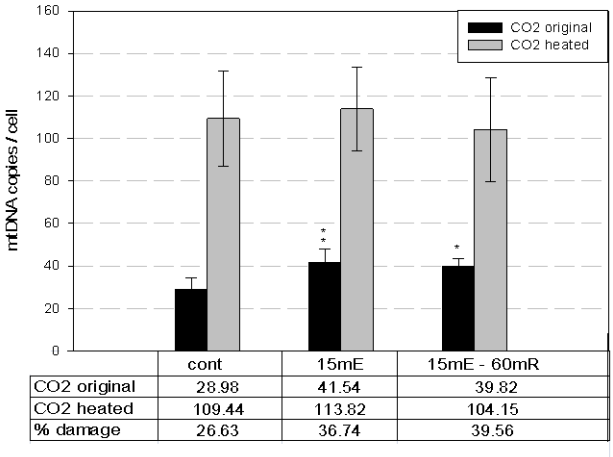

	cont	15mE	15mE - 60mR
CO2 original	28.98	41.54	39.82
CO2 heated	109.44	113.82	104.15
% damage	26.63	36.74	39.56

A **B**

Figure 5 mtDNA damage response after H_2O_2 challenge experiment.

Two experiments were performed to detect the endogenous damage level, induced damage by H_2O_2 treatment and repair capacity of white blood cells from healthy volunteers. (A) Lymphocytes were isolated from the fresh blood of three volunteers and frozen for storage. The lymphocytes were split into three groups, untreated control (n=3), 15 min of exposure to 120 μM H_2O_2 (n=3), and 15 min of exposure + 60 min recovery (n=2). (B) Blood from six healthy male volunteers were collected and frozen at -80^{o}C for storage. The whole blood sample of each volunteer was thawed, incubated in RPMI-1640/FBS medium and separated into three groups: untreated control, 15 min. of exposure to 120 μM H_2O_2, and 15 min of exposure to 120 μM H_2O_2 + 60 min recovery. (*=$p<0.05$, **=$p<0.01$)

Chapter 3

Differential mtDNA damage responses in prostate cancer cells with different metastatic potential

Authors: Chan, S.W., J. Chen, S. Chevalier, and J.Z. Chen

Manuscript in preparation

Connecting statement

In the previous chapter, we developed a new approach for assessing systemic oxidative stress using mtDNA from circulating lymphocytes which may be useful in epidemiological studies of prostate cancer risk and progression. In this chapter, we investigated dynamic mtDNA damage responses to induced oxidative stress in two isogenic prostate cancer cell lines with different metastatic potential. This study may offer new insights into the underlying mechanisms of prostate cancer progression.

Contributions

- MtDNA analysis of LNCaP and C4-2 treated with H_2O_2 performed by Jinsong Chen
- MtDNA analysis of C4-2 treated with H_2O_2 with and without administration of antioxidant NAC performed by Sam W. Chan
- MTT assay and fluorescent microscopy experiment performed by Nadia Passarelli and Sam W. Chan
- Supervisor: Junjian Z. Chen
- Co-supervisor: Simone Chevalier

5.1 Abstract

Prostate cancer cell line C4-2 is an isogenic clone isolated from androgen-responsive LNCaP cells. Unlike its parental cell line, C4-2 does not respond to androgen and exhibits increased metastatic potential. New evidence suggests that mtDNA aberrations in C4-2 cell may play a critical role in the aggressive phenotype. To understand the molecular mechanisms of this phenomenon, we propose to investigate mtDNA responses to induced oxidative stress in cultured cells. We hypothesized that mtDNA from LNCaP and C4-2 cells may respond differently to oxidative stress and that such differences may be associated with aggressive phenotypes in prostate cancer. Using the real-time PCR approach, we demonstrated a dynamic mtDNA response to oxidative stress in both cancer cell lines upon H_2O_2 treatment. It involved early mtDNA damage followed by repair activity or copy number reduction. We showed that LNCaP cells were more resistant to oxidative damage induced by 120 and 240 μM H_2O_2. Early mtDNA damage in LNCaP cells was repaired rapidly at low dose, but took 24 h to start recovering at high dose. In contrast, C4-2 cells were more susceptible to oxidative damage. Extensive mtDNA damage was induced at low dose of H_2O_2 (120 μM) in C4-2 cells, such that it was not repaired but instead, led to a 50% copy number reduction long after initial treatment. Interestingly, NAC antioxidant could partially prevent short-term mtDNA damage and enhance long-term repair activity in C4-2 cells. We conclude that the C4-2 cells are more susceptible to induced mtDNA damage than LNCaP cells. The increased susceptibility to oxidative damage may be caused by enhanced cellular ROS levels and mitochondrial dysfunction associated with more metastatic cancer cells.

5.2 Introduction

Prostate cancer is the most common cancer in men and the third leading cause of cancer death in Canada. Unfortunately, the primary causes leading to prostate malignancy are still poorly understood, but epidemiological studies have identified several risk factors for prostate cancer such as age, smoking, diet, ROS and single-nucleotide polymorphisms (SNPs) in metabolic and repair genes associated with oxidative stress [8-10]. In addition, increasing evidences suggest that the prostate may be particularly vulnerable to oxidative stress. The roles of ROS in cells are multifaceted. At low levels, ROS promote cell proliferation through activation of growth signalling pathways [23]. At high levels, ROS subject the cell to a state of oxidative stress, which may damage DNA, proteins and lipids, leading to mutation and cell toxicity [24-25]. For example, more than 2-fold increases in common oxidative DNA lesions were detected in prostate cancer *vs*. normal tissues [49]. On the other hand, antioxidants such as vitamin E and selenium appear to protect against prostate cancer [111-112].

The mitochondrion is a vital organelle that is responsible for energy production through oxidative phosphorylation, but also for the production of ROS, by-products of cellular respiration. Almost 80 years ago, Warburg coined the term "aerobic glycolysis" when he observed that cancer cells rely heavily on glycolysis for obtaining ATP when ATP generation from mitochondrial respiration was crippled [62]. Mitochondrial defects may be central to cancer cell biology and are closely associated with changes in mtDNA. MtDNA is a 16,569 bp circular DNA that is maintained semi-autonomously in the mitochondria and exists in multiple copies in a cell. It contains a main regulatory region (the D-loop) and 37 genes encoding 13 polypeptides involved in the ETC [55-56]. Due to its close proximity to the ETC and lack of histone protection, mtDNA is susceptible to

oxidative injury [57-60]. In fact, numerous studies have identified frequent somatic mutations in prostate cancer mtDNA [68-72]. Additionally, oxidative injury disrupts mtDNA structure integrity, which is crucial to normal mitochondrial function. The supercoiled structure of mtDNA is its functional form and is required for mtDNA replication and transcription. Single or double strand breaks due to oxidative damage convert the supercoiled form into relaxed forms. Equilibrium exists between the amount of relaxed and supercoiled structures since the damage is constantly repaired, but the accumulation of strand breaks may lead to the degradation of mtDNA molecules [84]. Chen *et al.* have developed a novel real-time PCR method for quantifying these different forms of mtDNA, which would help us assess mtDNA damage and total mtDNA copy in prostate cancer cells [109].

LNCaP and C4-2 are isogenic prostate cancer cells. LNCaP is a widely used prostate cancer cell line which is androgen-sensitive. While still expressing androgen-receptors, C4-2 cells are androgen-insensitive. The C4-2 cell line was generated from inoculation of LNCaP cells in a castrated mouse [113]. C4-2 cells are highly aggressive and metastasize readily to the bone [113]. Higuchi *et al.* have reported that C4-2 exhibited reduced total mtDNA copy and increased mtDNA deletions when compared to LNCaP [114]. These mtDNA aberrations inhibited mitochondrial cellular respiration in C4-2 cells by approximately 75% in comparison to LNCaP when measuring oxygen consumption. Furthermore, they have reported that LNCaP cells with depleted mtDNA resulted in the loss of androgen-responsiveness, while reintroduction of normal mtDNA in mtDNA-free LNCaP clones recovered androgen-responsiveness. These results suggest that mtDNA aberrations may be responsible for androgen-insensitivity and increased

metastasis in C4-2 cells. Thus, it would be important to study mechanisms of mtDNA responses to oxidative damage.

In this study, we hypothesize that mtDNA from LNCaP and C4-2 cells respond differently to oxidative stress, which can be detected using a novel real-time PCR method. We further hypothesize that antioxidants may prevent or reduce mtDNA damage in the cells. To confirm our hypothesis, (1) mtDNA damage, repair and total copy were quantified in LNCaP and C4-2 cells after H_2O_2 treatment, and (2) the effects of N-acetylcysteine (NAC) antioxidant on mtDNA damage response were analyzed in C4-2 cells treated with H_2O_2.

5.3 Material and Methods

5.3.1 Cell culture

2 to 2.5 x 10^6 LNCaP and C4-2 prostate cancer cells were cultured, each in 100 mm dishes with RPMI media 1640 (GIBCO) supplemented with 10% FBS (GIBCO) and 1% penicillin-streptomycin (GIBCO). LNCaP cells were cultured in 1% PLL (Sigma) coated dishes, while C4-2 cells were cultured in regular dishes. They were incubated at 37^{o}C with 5% CO_2 (Refer to chapter 1 of this thesis).

5.3.2 H_2O_2 challenge on LNCaP cells for mtDNA analysis

LNCaP cells were seeded 48 h prior to treatment. For exposure experiments, duplicate dishes of LNCaP cells were treated with 120 μM and 240 μM H_2O_2 solutions in serum-free medium for 5, 15, and 60 min. For recovery experiments, duplicate dishes of LNCaP cells were first treated with 120 μM and 240 μM H_2O_2 solutions in serum-free medium

for 60 min, and then allowed to recover in fresh complete medium for 2 or 24 h. The cells were collected by trypsin digestion; the cell pellets were washed down with PBS and stored at -80^{o}C prior to mtDNA analysis.

5.3.3 H_2O_2 challenge on C4-2 cells for mtDNA analysis

C4-2 cells were seeded 24 h prior to treatment. For exposure experiments, duplicate dishes of C4-2 cells were treated with 120 μM H_2O_2 solution in serum-free medium for 5, 15, and 60 min. For recovery experiments, duplicate dishes of C4-2 cells were first treated with 120 μM H_2O_2 solutions in serum-free medium for 60 min, and then allowed to recover in fresh complete medium for 6 and 24 h. The cells were collected by trypsin digestion; the cell pellets were washed down with PBS and stored at -80^{o}C prior to mtDNA analysis.

5.3.4 Nuclear DNA and mtDNA extraction

Genomic nuclear and mitochondrial DNA were extracted with the QIAGEN Blood & Cell Culture DNA Kit (Qiagen) with a few minor modifications to preserve mtDNA (refer to chapter 1 of this thesis). Concentrations of the DNA stock solutions from samples were quantified with Quant-iT PicoGreen dsDNA Assay Kit (Invitrogen) according to the proposed protocol (refer to chapter 1 of this thesis).

5.3.5 DNA template and standard preparation for real-time PCR analysis

From DNA stock solutions, 5 ng/μl and 1 ng/μl DNA templates were prepared in Tris/EDTA buffer (pH 8.0 ± 0.1, Fisher). The 5 ng/μl DNA templates were used for the quantification of nuclear markers. The 1 ng/μl DNA templates were split into two equal

halves. One half was left unmodified for the quantification of relaxed mtDNA. The other half was pre-treated to heat at 95°C for 6 min and was used for the quantification of total mtDNA content. 5-point DNA standard solutions (5X serial dilution) were made from the untreated control sample of each cell line. (Refer to chapter 1 of this thesis)

5.3.6 MtDNA damage analysis with real-time PCR

MyIQ Single Color Real-Time PCR Detection System (Bio-Rad) was used to perform relative amplification analysis. MtDNA and nuclear DNA markers, primers listed in Table 4, were used for real-time PCR amplification with SYBR Green Supermix (Bio-Rad). DNA templates and standards were analyzed in triplicate with the following PCR program: 95°C for 3 min, 30-40 cycles of 95°C for 20 sec followed by 61°C for 30 sec. A melt curve analysis was performed after amplification (Refer to chapter 1 of this thesis). Relative amplification analysis was performed based on the equation from Pfaffl [115]:

$$R = \frac{\left(Efficiency_{\ target\ gene}\right)^{\Delta CP\,\text{target}\left(Mean\,Control - Mean\,sample\right)}}{\left(Efficiency_{\ reference\,gene}\right)^{\Delta CP\,ref\left(Mean\,Control - Mean\,sample\right)}}. \qquad \textbf{Equation 1}$$

5.3.7 MtDNA analysis experiment in C4-2 cells pre-treated with an anti-oxidant

C4-2 cells were pre-treated with 4 mM of NAC in serum-free medium (Sigma-Aldrich) and incubated for 30 min at 37°C before treatment. For the exposure experiments, duplicate dishes of NAC pre-treated and NAC-free C4-2 were treated with 120 μM H_2O_2 for 1 h in serum-free medium. For the recovery experiments, they were treated for 1 h and allowed to recover in fresh complete medium for 2 h and 24 h. MtDNA analysis was performed as described previously in "4.2.6 MtDNA damage analysis with real-time PCR".

5.3.8 Data analysis

All statistical analyses were performed with the aid of Graphpad Prism version 4 software. Unless specified otherwise, the data were analyzed with one-way ANOVA.

Table 4 Chapter 3 - Primer Sequences

Gene	Forward primer 5'-3'	Reverse primer 5'-3'
CO2 (mtDNA)	CCCCACATTAGGCTTAAAAACAGAT	TATACCCCCGGTCGTGTAGCGGT
D-loop (mtDNA)	TATCTTTTGGCGGTATGCACTTTTAACAGT	TGATGAGATTAGTAGTATGGGAGTGG
β-actin	TCACCCACACTGTGCCCATCTACGA	CAGCGGAACCGCTCATTGCCAATGG
β-globin	GTGCACCTGACTCCTGAGGAGA	CCTTGATACCAACCTGCCCAG

5.4 Results

5.4.1 MtDNA damage responses induced by H_2O_2 in LNCaP

LNCaP cells were treated with 120 and 240 μM of H_2O_2 for 5, 15 and 60 min to induce mtDNA damage. For recovery, the cells were first treated for 60 min and then allowed to recover in fresh complete medium for 2 and 24 h. Total genomic DNA was extracted from the cells and real-time PCR amplification of the CO2 marker was used to quantify the original (CO2 ori) and pre-heated (CO2-heated) DNA templates of each sample. An increase in the amplification signal from the original DNA template would signify that the amount of relaxed mtDNA has increased. This in turn suggests that there is an increase in mtDNA damage. In contrast, if the total copy remains the same and there is a decrease in relaxed mtDNA detected from the original template, it would suggest that the damaged mtDNA was repaired. Total copy can be quantified with the pre-heated DNA templates, since heat pre-treatment will have converted all of mtDNA into the relaxed form. During the first 5 min at 120 μM of H_2O_2 treatment, mtDNA damage detected from the relaxed mtDNA of the original template increased by 1.25-fold over the control level ($p<0.01$) (Figure 6A). As the time of treatment increased, the amount of relaxed mtDNA also increased by 1.5-fold for 15 min treatment when compared to the control. ($p<0.01$) The amount of relaxed mtDNA then decreased starting from 60 min of treatment (1.28-fold compared to the control, $p<0.01$), and because total copy detected from the pre-heated DNA templates remained stable, it suggested that mtDNA repair activity was taking place. MtDNA repair was also observed at 2 h recovery, as the amount of relaxed mtDNA decreased further to around the control level. At 24 h of recovery, the amount of relaxed mtDNA was reduced to 0.9-fold of the control level

($p<0.05$). There were few minor variations in total mtDNA copy ($p>0.05$), but it remained stable across all time points.

In the first 5 min of 240 μM of H_2O_2 treatment, the mtDNA damage detected from the relaxed mtDNA of the original template increased by 2.1-fold over control level ($p<0.01$) (Figure 6 B). Interestingly, the amplification signal from the original template is the same, or slightly more, than the pre-heated template's, suggesting that all mtDNA was relaxed. At 15 min of treatment, relaxed mtDNA remained at 2-fold higher than control level ($p<0.01$). At 60 min of treatment, all mtDNA remained relaxed and there was also a 32% decrease in total mtDNA copy ($p<0.01$) compared to the control. This loss of total mtDNA copy suggested that mtDNA was degraded. At 2 h of recovery, more than half of the total mtDNA copy was lost. After 24 h of recovery, total mtDNA copy was quantified at 0.6-fold of the control sample ($p<0.01$), but this represented a 1.3-fold increase compared to the 2 h recovery time point, suggesting a start in the repair process. With this experiment we detected a very dynamic dose and time-dependent mtDNA response to oxidative stress.

5.4.2 MtDNA damage responses induced by H_2O_2 in C4-2 cells

C4-2 cells were treated with 120 μM of H_2O_2 for 5, 15 and 60 min to induce mtDNA damage. For recovery, the cells were first treated for 60 min and then allowed to recover in fresh complete medium for 6 and 24 h. Extensive mtDNA damage was detected from the 1.8-fold increase in relaxed mtDNA from the original template when compared to the control (Figure 6C). At 15 min of treatment, the amount of relaxed mtDNA increased by 2.3 fold over the control level. At this point, the amount of relaxed mtDNA was the same as the detected total mtDNA copy, suggesting that all mtDNA has been relaxed. Starting

from 60 min of treatment, there was a loss of total mtDNA copy, 0.7-fold compared to the control. This suggested that mtDNA was degraded. After 24 h of recovery, almost half of the mtDNA content was lost. This behaviour of C4-2 cells treated at a low dose of H_2O_2 was very similar to LNCaP cells treated at the high dose. This suggests that the more metastatic C4-2 cells may be more susceptible to oxidative stress than LNCaP cells.

5.4.3 Effects of N-acetylcysteine (NAC) anti-oxidant on C4-2 cells

The mtDNA damage observed in the previous analysis was induced by an exogenous source of oxidative stress, and we suspected that an antioxidant may prevent or reduce mtDNA damage. To test this hypothesis, we treated C4-2 cells with 4 mM of antioxidant NAC for 30 min before exposing the cells to 120 μM of H_2O_2 for 1 h, and then allowed the cells to recover for 2 h and 24 h. Alongside this experiment, NAC-free C4-2 cells were also treated and analyzed. Similar levels of relaxed mtDNA and total mtDNA copy were detected from the control samples without H_2O_2 treatment of either NAC-treated or NAC-free cells, suggesting that NAC pre-treatment did not affect mtDNA damage level nor the total mtDNA copy. At 1 h of treatment for the NAC-free cells, an increase of 1.7-fold in relaxed mtDNA was detected compared to the control ($p<0.05$). A decrease in total mtDNA copy compared to the control was also observed, but the difference was not significant. It is interesting to note that all mtDNA was relaxed for this sample at 1 h of treatment. In comparison, with NAC-treated cells, a 1.6 fold increase in relaxed mtDNA was detected when compared to the control, but the total mtDNA copy remained stable at the control level. When allowed to recover for 2 h, the NAC-free cells lost 48% total mtDNA copy compared to the control ($p<0.01$), while NAC pre-treated cells lost 18% compared to control ($p<0.05$). After 24 h of recovery, the total mtDNA copy for NAC-free cells increased slightly to 0.65-fold of control ($p<0.01$), but the total mtDNA copy

from NAC-treated cells returned to control level. Antioxidant pre-treatment in C4-2 cells seemed to have reduced the damage to mtDNA, and these cells had a better outcome after 24 h of recovery than the ones without pre-treatment. Data from duplicate experiments were pooled and analyzed together.

5.5 Discussion

In this study, we have revealed a very dynamic process in mtDNA damage responses to oxidative stress in two isogenic cell lines with different metastatic potentials. The LNCaP cells which are androgen-responsive, exhibited dose and time-dependent mtDNA damage upon H_2O_2 treatment. In fact, significant mtDNA damage was observed almost immediately after H_2O_2 treatment. At low dose, the induced damage could be repaired within 2 h recovery; however, at high dose, it led to degradation and reduction in total copy number. As for the androgen-insensitive cell line, C4-2, it exhibited a different response pattern in comparison to LNCaP cells. Even at low dose of H_2O_2 treatment, we observed significantly more initial damage in mtDNA of C4-2 cells. The extensive damage could not be repaired and, as a result, led to a significant reduction in total mtDNA copy number over a period of 24 h. Therefore, the androgen-insensitive and more metastatic C4-2 cells appear to be more susceptible to oxidative damage. This differential damage response between the two prostate cancer cell lines is consistent with the observation of mtDNA alterations in prostate cancer progression reported by Higuchi *et al*. [114] To further explore the molecular mechanisms underlining the differential damage response in the two cell lines, their redox activities were analyzed using MTT assay in another study. Consistent with mtDNA damage response, an increased redox toxicity was detected in C4-2 cells, which led to significantly more growth inhibition

over time than LNCaP cells when stressed by different doses of H_2O_2 (data attached in appendices, Figure 8). Furthermore, we have determined earlier the exact mtDNA copy numbers in untreated C4-2 and LNCaP cells at 1495 and 3086 copies/cell, respectively, which seem to substantiate the observations made by Higuchi *et al.* on reduced mtDNA content in C4-2 [refer to chapter 2 of this thesis]. Taken together, altered mtDNA content and differential damage response between C4-2 and LNCaP prostate cancer cells provide new evidence to support a critical role played by mitochondrial dysfunction in prostate carcinogenesis and progression.

The increased susceptibility of C4-2 cells to oxidative damage may reflect a cascade mechanism in ROS interaction in cancer cells. Acute mtDNA damage was observed in C4-2 cells in the first few minutes of treatment, followed by a sustained mtDNA damage increase beyond 24 h after treatment. Since the reported H_2O_2 half-life in cells is very short, we suspected there was a secondary ROS production, triggered by the initial H_2O_2 treatment, which in turn contributed to the sustained mtDNA damage and copy number reduction observed in C4-2 cells. In order to confirm this possibility, we carried another study using dihydroethidium (DHE) probes and fluorescent microscopy to detect superoxide production (data attached in appendices, Figure 9) and indeed observed a secondary superoxide production in C4-2 cells after H_2O_2 treatment. The mechanism underlining this phenomenon is not clear from the limited data. It is possible that an acute H_2O_2 exposure in cancer cells may trigger a secondary superoxide production inside the cell, leading to a fenton reaction and accumulation of hydroxyl radicals. This chain of ROS conversions may explain the sustained mtDNA damage in C4-2 cells. On the other hand, NAC had preventive effects on mtDNA damage in C4-2 cells. The antioxidant NAC is a precursor for the synthesis of glutathione which is a key peptide used by

glutathione peroxidase in cellular antioxidant defence. In our findings, a significant reduction in short-term mtDNA damage and an enhanced long-term repair activity were observed in C4-2 cells when NAC was administered in cell culture. Hence, the preventive effects offered by NAC antioxidant not only suggests a mechanism underlining the increased susceptibility of C4-2 cells to oxidative damage, but may also have implications in prostate cancer prevention and treatment. Additional work is required to address the relationship between mtDNA dysfunction, differential susceptibility to oxidative stress and metastatic potential in prostate cancer cells.

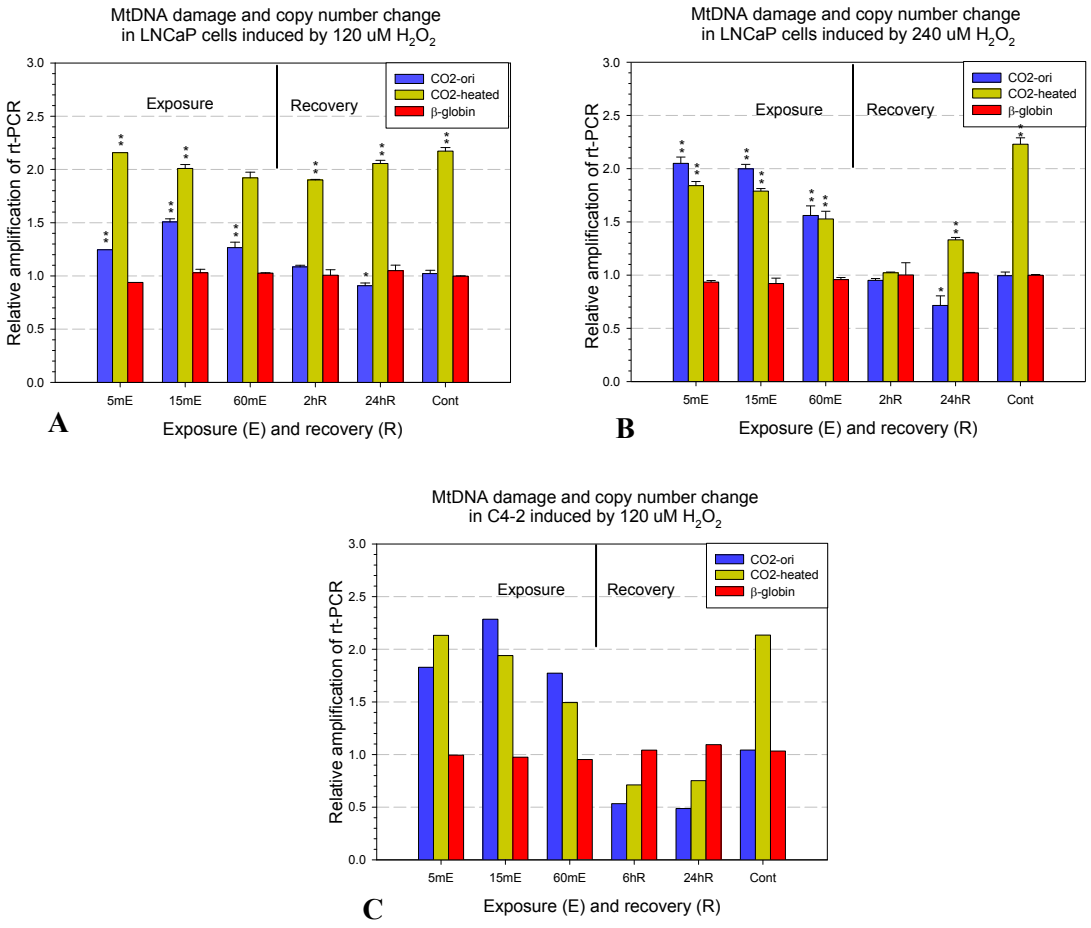

Figure 6 MtDNA damage and copy number change in LNCaP and C4-2 cells induced by H_2O_2 exposure.

LNCaP cells were treated with 120 (A) or 240 μM H_2O_2 (B) in serum free medium for 5, 15 and 60 min, respectively, to induce mtDNA damage. For the recovery experiment, LNCaP cells were first treated with 120 or 240 μM H_2O_2 for 60 min, then allowed to recover in fresh medium for 2 and 24 h respectively. C4-2 cells were treated with120 μM H_2O_2 for both exposure and recovery experiments (C). MtDNA (CO2) and nuclear DNA (β-actin and β-globin) markers were used for real-time PCR using total genomic DNA isolated from each sample. The CO2 marker was used to analyze the original and heat pre-treated (95^{o}C for 6 min) DNA template to determine the quantity of relaxed (CO2-ori) or total (CO2-heated) mtDNA from each sample. Two additional nuclear markers were analyzed: β-actin was used as the reference gene to normalize results and β-globin, for monitoring loading.

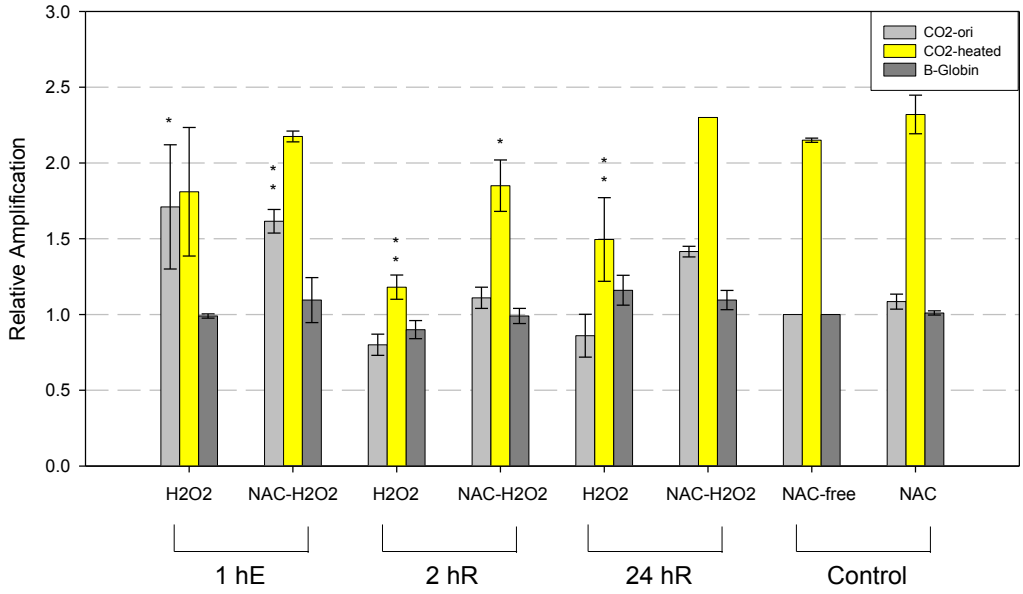

Figure 7 Effects of NAC antioxidant on mtDNA damage and total mtDNA copy in C4-2 cells.

C4-2 cells were pre-treated with 4 mM NAC for 30 min before H_2O_2 treatment. For exposure, both the pre-treated and non pre-treated cells were treated with 120 μM H_2O_2 for 1 h. For recovery, the cells were allowed to recover for 2 and 24 h after the 1 h of treatment. At each time point, the results of non-pre-treated (left) and NAC pre-treated (right) cells were grouped together for comparison. The CO2 marker was used to analyze the original or heat pre-treated (95^{o}C for 6 min) DNA template to determine the quantity of initial relaxed (CO2-ori) or total (CO2-heated) mtDNA from each sample. Two additional nuclear markers were analyzed, β -actin as the reference gene to normalize results, and β-globin, for monitoring loading.

6. Conclusions

In this manuscript-based thesis, we have studied mtDNA as a surrogate to oxidative stress in three different perspectives: method development, detection of systemic oxidative stress in circulating lymphocytes and detection of differential mtDNA damage responses in isogenic cancer cell lines.

In the first chapter, we developed a step-by-step protocol for a novel method for the quantitative analysis of mtDNA damage, repair and total copy change using real-time PCR. This standardized method overcomes many limitations of existing methods such as the semi-quantitative nature of gel electrophoresis and the lack of information on mtDNA structure using long PCR method. Many improvements were made to the method since it was first published by Chen et al. [84]. It was observed that artificial damages were introduced when mtDNA was subjected to heat of 95^{o}C for a prolonged period of time [84]. We hypothesized that by shortening the time required by the real-time PCR procedure for heating the samples, mainly the initial heat-activation step, there would be decrease in artificial damage introduced. Hence, we improved the method by establishing a fast procedure in real-time PCR, which significantly reduces the amount of experimental artifacts up to 34.5% associated with the previous method. This improvement in sensitivity makes it possible to measure endogenous mtDNA damage in cells more accurately.

In the second chapter, we further developed a new approach to detect systemic oxidative stress by absolute quantification of mtDNA markers in circulating lymphocytes and whole blood. We suggest that oxidative stress is not only a characteristic of prostate cancer cells, but also a distinctive feature of the circulating cells in prostate cancer patients. High levels of systemic oxidative stress have been associated with increased

prostate cancer risk [36-37], and with aggressive forms of prostate cancers [94]. Consequently, our non-invasive and quantitative approach may prove to be useful in epidemiological studies for assessing prostate cancer risks among the population, or in studies for aggressive prostate cancer progression. In the process of developing this new approach, we have outlined a detailed protocol which was described in three main parts: 1) nuclear DNA and mtDNA standard preparation, 2) DNA sample preparation, and 3) real-time PCR analysis of mtDNA damage and total copy number. In our initial test of the new approach, we have demonstrated that lymphocytes from healthy men have a significantly lower total mtDNA copy number and endogenous levels of damage than in prostate cancer cells. As expected, these results are in agreement with the notion from the literature that mtDNA content varies greatly between cell types. Furthermore in our damage response experiments, we observed that mtDNA in lymphocytes exhibited significantly induced damage after H_2O_2 exposure, but lack repair activity in ex-vivo challenge test. In this second chapter, we propose that our new non-invasive approach may be a valuable addition for detecting systemic oxidative stress, since it offers several advantages over existing methods. The new approach allows quantification of precise mtDNA content, endogenous damage levels and induced stress responses simultaneously. These multiple endpoints allow for flexible and methodical analyses of systemic oxidative stress.

In the third chapter, we investigated the dynamic mtDNA damage responses to oxidative stress in two isogenic prostate cancer cell lines with different metastatic potentials, which would offer new insights into the underlying mechanisms of prostate cancer progression. We not only detected vastly different amount of mtDNA content between LNCaP and C4-2 cells (LNCaP has over 2-fold more than C4-2), but when treated with the same

amount of oxidative stress, we measured a significant increase in the amount of mtDNA damage and total mtDNA copy reduction in C4-2 cells when compared to LNCaP cells. This suggests that the more metastatic and androgen-insensitive C4-2 cells are more susceptible to oxidative stress, probably through a cascade mechanism in secondary production of toxic ROS. This differential damage response between the two prostate cancer cell lines is also consistent with reported observations on mtDNA alterations in the prostate cancer progression of LNCaP and C4-2 cells [114]. In agreement with our mtDNA results, MTT data also supported the observed differential damage response to H_2O_2 between the two cell lines. We detected increased redox toxicity in C4-2 cells that led to a significant cell toxicity and growth inhibition over time when compared to LNCaP cells. Taken altogether, our results on altered mtDNA content and differential damage response between LNCaP and C4-2 cells support the notion that mitochondrial dysfunction may be a key player in prostate carcinogenesis and progression [21, 62, 73]. One notable observation is that the administration of the NAC antioxidant partially prevented and reduced mtDNA damage induced by H_2O_2 treatment and allowed an enhanced long-term repair capacity in C4-2 cells. Ultimately, further studies of the differential mtDNA damage response between LNCaP and C4-2 cells, the enhanced susceptibility to oxidative stress of C4-2 cells, and the intricate balance between oxidants and antioxidant systems may provide new insights on the mechanism of prostate cancer progression.

Taken together, mtDNA may serve as a sensitive molecular marker to detect either oxidative damage from patients' local/tissue specific cancer cells or systemic oxidative stress from their circulating blood cells**.** The results from the studies not only provide new understanding on the role of oxidative stress in prostate carcinogenesis, but also

provide sensitive markers for clinical analysis of prostate cancer risk and progression. For future directions, there are two potential facets that we can explore: 1) using our new approach for systemic oxidative stress we can conduct an epidemiological study between a healthy population and prostate cancer patients, 2) to expand our work with the prostate cancer cell lines and investigate the biological pathways and the underlining mechanisms responsible for the differential oxidative stress responses observed between LNCaP and C4-2 prostate cancer cells. For the epidemiological study, the goal would be to test the hypothesis that either the variation in mtDNA content, endogenous damage, and or damage responses measured from lymphocytes can distinguish populations with a higher risk of prostate cancer and progression. The same approach could be applied to other cancers as well, notably renal and bladder cancers. For expanding the cell line work, it would be worthwhile to confirm our results with additional isogenic prostate cancer cell lines with different metastatic potentials such as PC-3 and LN4 (LN4's metastatic potential > PC-3's).

7. References

1. Hayward, S.W. and G.R. Cunha, *The prostate: development and physiology.* Radiol Clin North Am, 2000. **38**(1): p. 1-14.
2. Aumuller, G. and J. Seitz, *Protein secretion and secretory processes in male accessory sex glands.* Int Rev Cytol, 1990. **121**: p. 127-231.
3. Young, C.Y., et al., *Hormonal regulation of prostate-specific antigen messenger RNA in human prostatic adenocarcinoma cell line LNCaP.* Cancer Res, 1991. **51**(14): p. 3748-52.
4. Stamey, T.A., et al., *Prostate-specific antigen as a serum marker for adenocarcinoma of the prostate.* N Engl J Med, 1987. **317**(15): p. 909-16.
5. McNeal, J.E., *Normal anatomy of the prostate and changes in benign prostatic hypertrophy and carcinoma.* Semin Ultrasound CT MR, 1988. **9**(5): p. 329-34.
6. *Canadian Cancer Society*. [cited 2009; Available from: http://www.cancer.ca.
7. *National Cancer Institute*. 2009 [cited 2009; Available from: http://www.cancer.gov.
8. Rose, D.P., A.P. Boyar, and E.L. Wynder, *International comparisons of mortality rates for cancer of the breast, ovary, prostate, and colon, and per capita food consumption.* Cancer, 1986. **58**(11): p. 2363-71.
9. Fair, W.R., N.E. Fleshner, and W. Heston, *Cancer of the prostate: a nutritional disease?* Urology, 1997. **50**(6): p. 840-8.
10. Xu, J., et al., *Associations between hOGG1 sequence variants and prostate cancer susceptibility.* Cancer Res, 2002. **62**(8): p. 2253-7.
11. Cancel-Tassin, G. and O. Cussenot, *Prostate cancer genetics.* Minerva Urol Nefrol, 2005. **57**(4): p. 289-300.
12. Smith, J.R., et al., *Major susceptibility locus for prostate cancer on chromosome 1 suggested by a genome-wide search.* Science, 1996. **274**(5291): p. 1371-4.
13. Damber, J.E. and G. Aus, *Prostate cancer.* Lancet, 2008. **371**(9625): p. 1710-21.
14. Deutsch, E., et al., *Environmental, genetic, and molecular features of prostate cancer.* Lancet Oncol, 2004. **5**(5): p. 303-13.
15. Dong, J.T., *Prevalent mutations in prostate cancer.* J Cell Biochem, 2006. **97**(3): p. 433-47.
16. Edwards, S.M. and R.A. Eeles, *Unravelling the genetics of prostate cancer.* Am J Med Genet C Semin Med Genet, 2004. **129C**(1): p. 65-73.
17. Porkka, K.P. and T. Visakorpi, *Molecular mechanisms of prostate cancer.* Eur Urol, 2004. **45**(6): p. 683-91.
18. Amundadottir, L.T., et al., *A common variant associated with prostate cancer in European and African populations.* Nat Genet, 2006. **38**(6): p. 652-8.
19. Parkin, D.M. and C.S. Muir, *Cancer Incidence in Five Continents. Comparability and quality of data.* IARC Sci Publ, 1992(120): p. 45-173.
20. Adlercreutz, H. and W. Mazur, *Phyto-oestrogens and Western diseases.* Ann Med, 1997. **29**(2): p. 95-120.
21. Wallace, D., *A mitochondrial paradigm of metabolic and degenerative diseases, aging, and cancer: a dawn for evolutionary medicine.* Annu Rev Genet, 2005. **39**: p. 359-407.
22. Davies, K.J., *The broad spectrum of responses to oxidants in proliferating cells: a new paradigm for oxidative stress.* IUBMB Life, 1999. **48**(1): p. 41-7.
23. Benhar, M., D. Engelberg, and A. Levitzki, *ROS, stress-activated kinases and stress signaling in cancer.* EMBO Rep, 2002. **3**(5): p. 420-5.

24. Martindale, J.L. and N.J. Holbrook, *Cellular response to oxidative stress: signaling for suicide and survival.* J Cell Physiol, 2002. **192**(1): p. 1-15.
25. Chen, J.Z. and F.F. Kadlubar, *A new clue to glaucoma pathogenesis.* Am J Med, 2003. **114**(8): p. 697-8.
26. Gutteridge, J.M. and B. Halliwell, *Comments on review of Free Radicals in Biology and Medicine, second edition, by Barry Halliwell and John M. C. Gutteridge.* Free Radic Biol Med, 1992. **12**(1): p. 93-5.
27. Hayes, J.D. and L.I. McLellan, *Glutathione and glutathione-dependent enzymes represent a co-ordinately regulated defence against oxidative stress.* Free Radic Res, 1999. **31**(4): p. 273-300.
28. Demple, B. and L. Harrison, *Repair of oxidative damage to DNA: enzymology and biology.* Annu Rev Biochem, 1994. **63**: p. 915-48.
29. Vander, A., J. Sherman, and D. Luciano, eds. *Human physiology: the mechanisms of body function*. 8th ed. ed., ed. T. Kane. 2001, McGraw-Hill: New York.
30. Griffiths, H.R., *ROS as signalling molecules in T cells--evidence for abnormal redox signalling in the autoimmune disease, rheumatoid arthritis.* Redox Rep, 2005. **10**(6): p. 273-80.
31. Gibson, G.E. and H.M. Huang, *Oxidative processes in the brain and non-neuronal tissues as biomarkers of Alzheimer's disease.* Front Biosci, 2002. **7**: p. d1007-15.
32. Gibson, G.E. and H.M. Huang, *Oxidative stress in Alzheimer's disease.* Neurobiol Aging, 2005. **26**(5): p. 575-8.
33. Leuner, K., et al., *Enhanced apoptosis, oxidative stress and mitochondrial dysfunction in lymphocytes as potential biomarkers for Alzheimer's disease.* J Neural Transm Suppl, 2007(72): p. 207-15.
34. Czlonkowska, A., et al., *Immune processes in the pathogenesis of Parkinson's disease - a potential role for microglia and nitric oxide.* Med Sci Monit, 2002. **8**(8): p. RA165-77.
35. Barnes, P.J., S.D. Shapiro, and R.A. Pauwels, *Chronic obstructive pulmonary disease: molecular and cellular mechanisms.* Eur Respir J, 2003. **22**(4): p. 672-88.
36. Lockett, K., et al., *DNA damage levels in prostate cancer cases and controls.* Carcinogenesis, 2006. **27**(6): p. 1187-93.
37. Waters, D., et al., *Noninvasive prediction of prostatic DNA damage by oxidative stress challenge of peripheral blood lymphocytes.* Cancer Epidemiol Biomarkers Prev, 2007. **16**(9): p. 1906-10.
38. Wei, Q., et al., *Reduced DNA repair capacity in lung cancer patients.* Cancer Res, 1996. **56**(18): p. 4103-7.
39. Saha, D., et al., *Quantification of DNA repair capacity in whole blood of patients with head and neck cancer and healthy donors by comet assay.* Mutat Res, 2008. **650**(1): p. 55-62.
40. Xing, J., et al., *Mitochondrial DNA content: its genetic heritability and association with renal cell carcinoma.* J Natl Cancer Inst, 2008. **100**(15): p. 1104-12.
41. Wu, M., et al., *Lymphocytic mitochondrial DNA deletions, biochemical folate status and hepatocellular carcinoma susceptibility in a case-control study.* Br J Nutr, 2009: p. 1-7.
42. Burdon, R.H., *Superoxide and hydrogen peroxide in relation to mammalian cell proliferation.* Free Radic Biol Med, 1995. **18**(4): p. 775-94.

43. Gupta, A., S.F. Rosenberger, and G.T. Bowden, *Increased ROS levels contribute to elevated transcription factor and MAP kinase activities in malignantly progressed mouse keratinocyte cell lines.* Carcinogenesis, 1999. **20**(11): p. 2063-73.
44. Behrend, L., G. Henderson, and R.M. Zwacka, *Reactive oxygen species in oncogenic transformation.* Biochem Soc Trans, 2003. **31**(Pt 6): p. 1441-4.
45. Dakubo, G., et al., *Altered metabolism and mitochondrial genome in prostate cancer.* J Clin Pathol, 2006. **59**(1): p. 10-6.
46. Jackson, A.L. and L.A. Loeb, *The contribution of endogenous sources of DNA damage to the multiple mutations in cancer.* Mutat Res, 2001. **477**(1-2): p. 7-21.
47. Ripple, M.O., et al., *Prooxidant-antioxidant shift induced by androgen treatment of human prostate carcinoma cells.* J Natl Cancer Inst, 1997. **89**(1): p. 40-8.
48. Costello, L.C. and R.B. Franklin, *The intermediary metabolism of the prostate: a key to understanding the pathogenesis and progression of prostate malignancy.* Oncology, 2000. **59**(4): p. 269-82.
49. Malins, D.C., et al., *Age-related radical-induced DNA damage is linked to prostate cancer.* Cancer Res, 2001. **61**(16): p. 6025-8.
50. Trzeciak, A.R., et al., *Cellular repair of oxidatively induced DNA base lesions is defective in prostate cancer cell lines, PC-3 and DU-145.* Carcinogenesis, 2004. **25**(8): p. 1359-70.
51. Fan, R., et al., *Defective DNA strand break repair after DNA damage in prostate cancer cells: implications for genetic instability and prostate cancer progression.* Cancer Res, 2004. **64**(23): p. 8526-33.
52. Nelson, W.G., A.M. De Marzo, and T.L. DeWeese, *The molecular pathogenesis of prostate cancer: Implications for prostate cancer prevention.* Urology, 2001. **57**(4 Suppl 1): p. 39-45.
53. DeWeese, T.L., A.M. Hruszkewycz, and L.J. Marnett, *Oxidative stress in chemoprevention trials.* Urology, 2001. **57**(4 Suppl 1): p. 137-40.
54. Palapattu, G.S., et al., *Prostate carcinogenesis and inflammation: emerging insights.* Carcinogenesis, 2005. **26**(7): p. 1170-81.
55. Anderson, S., et al., *Sequence and organization of the human mitochondrial genome.* Nature, 1981. **290**(5806): p. 457-65.
56. Clayton, D.A., *Transcription and replication of mitochondrial DNA.* Hum Reprod, 2000. **15 Suppl 2**: p. 11-7.
57. Richter, C., J.W. Park, and B.N. Ames, *Normal oxidative damage to mitochondrial and nuclear DNA is extensive.* Proc Natl Acad Sci U S A, 1988. **85**(17): p. 6465-7.
58. Mecocci, P., et al., *Oxidative damage to mitochondrial DNA shows marked age-dependent increases in human brain.* Ann Neurol, 1993. **34**(4): p. 609-16.
59. Hayakawa, M., et al., *Massive conversion of guanosine to 8-hydroxy-guanosine in mouse liver mitochondrial DNA by administration of azidothymidine.* Biochem Biophys Res Commun, 1991. **176**(1): p. 87-93.
60. Ames, B.N., M.K. Shigenaga, and T.M. Hagen, *Oxidants, antioxidants, and the degenerative diseases of aging.* Proc Natl Acad Sci U S A, 1993. **90**(17): p. 7915-22.
61. Graziewicz, M.A., M.J. Longley, and W.C. Copeland, *DNA polymerase gamma in mitochondrial DNA replication and repair.* Chem Rev, 2006. **106**(2): p. 383-405.
62. Warburg, O., *On the origin of cancer cells.* Science, 1956. **123**(3191): p. 309-14.

63. Penta, J.S., et al., *Mitochondrial DNA in human malignancy.* Mutat Res, 2001. **488**(2): p. 119-33.
64. Toyokuni, S., et al., *Persistent oxidative stress in cancer.* FEBS Lett, 1995. **358**(1): p. 1-3.
65. Dorward, A., et al., *Mitochondrial contributions to cancer cell physiology: redox balance, cell cycle, and drug resistance.* J Bioenerg Biomembr, 1997. **29**(4): p. 385-92.
66. Herrmann, P., et al., *Mitochondrial proteome: altered cytochrome c oxidase subunit levels in prostate cancer.* Proteomics, 2003. **3**(9): p. 1801-10.
67. Krieg, R.C., et al., *Mitochondrial proteome: cancer-altered metabolism associated with cytochrome c oxidase subunit level variation.* Proteomics, 2004. **4**(9): p. 2789-95.
68. Jeronimo, C., et al., *Mitochondrial mutations in early stage prostate cancer and bodily fluids.* Oncogene, 2001. **20**(37): p. 5195-8.
69. Chen, J., et al., *Extensive somatic mitochondrial mutations in primary prostate cancer using laser capture microdissection.* Cancer Res, 2002. **62**(22): p. 6470-4.
70. Chen, J., et al., *Simultaneous generation of multiple mitochondrial DNA mutations in human prostate tumors suggests mitochondrial hyper-mutagenesis.* Carcinogenesis, 2003. **24**(9): p. 1481-7.
71. Petros, J.A., et al., *mtDNA mutations increase tumorigenicity in prostate cancer.* Proc Natl Acad Sci U S A, 2005. **102**(3): p. 719-24.
72. Parr, R.L., et al., *Somatic mitochondrial DNA mutations in prostate cancer and normal appearing adjacent glands in comparison to age-matched prostate samples without malignant histology.* J Mol Diagn, 2006. **8**(3): p. 312-9.
73. Brandon, M., P. Baldi, and D.C. Wallace, *Mitochondrial mutations in cancer.* Oncogene, 2006. **25**(34): p. 4647-62.
74. Chan, S.W. and J.Z. Chen, *Measuring mtDNA damage using a supercoiling-sensitive qPCR approach.* Methods Mol Biol, 2009. **554**: p. 183-97.
75. Turrens, J.F. and A. Boveris, *Generation of superoxide anion by the NADH dehydrogenase of bovine heart mitochondria.* Biochem J, 1980. **191**(2): p. 421-7.
76. Richter, C., *Oxidative damage to mitochondrial DNA and its relationship to ageing.* Int J Biochem Cell Biol, 1995. **27**(7): p. 647-53.
77. Herrmann, P.C., et al., *Mitochondrial proteome: altered cytochrome c oxidase subunit levels in prostate cancer.* Proteomics, 2003. **3**(9): p. 1801-10.
78. Fliss, M., et al., *Facile detection of mitochondrial DNA mutations in tumors and bodily fluids.* Science, 2000. **287**(5460): p. 2017-9.
79. Parrella, P., et al., *Detection of mitochondrial DNA mutations in primary breast cancer and fine-needle aspirates.* Cancer Res, 2001. **61**(20): p. 7623-6.
80. Radloff, R., W. Bauer, and J. Vinograd, *A dye-buoyant-density method for the detection and isolation of closed circular duplex DNA: the closed circular DNA in HeLa cells.* Proc Natl Acad Sci U S A, 1967. **57**(5): p. 1514-21.
81. Robberson, D.L. and D.A. Clayton, *Replication of mitochondrial DNA in mouse L cells and their thymidine kinase - derivatives: displacement replication on a covalently-closed circular template.* Proc Natl Acad Sci U S A, 1972. **69**(12): p. 3810-4.
82. Bogenhagen, D. and D.A. Clayton, *Mechanism of mitochondrial DNA replication in mouse L-cells: introduction of superhelical turns into newly replicated molecules.* J Mol Biol, 1978. **119**(1): p. 69-81.
83. Clayton, D.A., *Replication of animal mitochondrial DNA.* Cell, 1982. **28**(4): p. 693-705.

84. Chen, J., F. Kadlubar, and J. Chen, *DNA supercoiling suppresses real-time PCR: a new approach to the quantification of mitochondrial DNA damage and repair.* Nucleic Acids Res, 2007. **35**(4): p. 1377-88.
85. Ayala-Torres, S., et al., *Analysis of gene-specific DNA damage and repair using quantitative polymerase chain reaction.* Methods, 2000. **22**(2): p. 135-47.
86. Pfaffl, M.W., *A new mathematical model for relative quantification in real-time RT-PCR.* Nucleic Acids Res, 2001. **29**(9): p. e45.
87. Chen, J. and F. Kadlubar, *Mitochondrial mutagenesis and oxidative stress in human prostate cancer.* J Environ Sci Health C Environ Carcinog Ecotoxicol Rev, 2004. **22**(1): p. 1-12.
88. Toyokuni, S., et al., *Persistent oxidative stress in cancer.* FEBS Lett, 1995. **358**(1): p. 1-3.
89. De Marzo, A., et al., *Human prostate cancer precursors and pathobiology.* Urology, 2003. **62**(5 Suppl 1): p. 55-62.
90. Bostwick, D., et al., *Human prostate cancer risk factors.* Cancer, 2004. **101**(10 Suppl): p. 2371-490.
91. Klein, E., G. Casey, and R. Silverman, *Genetic susceptibility and oxidative stress in prostate cancer: integrated model with implications for prevention.* Urology, 2006. **68**(6): p. 1145-51.
92. Naylor, S., *SNPs associated with prostate cancer risk and prognosis.* Front Biosci, 2007. **12**: p. 4111-31.
93. Wang, L., et al., *Polymorphisms in mitochondrial genes and prostate cancer risk.* Cancer Epidemiol Biomarkers Prev, 2008. **17**(12): p. 3558-66.
94. Yossepowitch, O., et al., *Advanced but not localized prostate cancer is associated with increased oxidative stress.* J Urol, 2007. **178**(4 Pt 1): p. 1238-43; discussion 1243-4.
95. Athas, W., et al., *Development and field-test validation of an assay for DNA repair in circulating human lymphocytes.* Cancer Res, 1991. **51**(21): p. 5786-93.
96. Cheng, L., et al., *Cryopreserving whole blood for functional assays using viable lymphocytes in molecular epidemiology studies.* Cancer Lett, 2001. **166**(2): p. 155-63.
97. Thirunavukkarasu, C. and D. Sakthisekaran, *Sodium selenite, dietary micronutrient, prevents the lymphocyte DNA damage induced by N-nitrosodiethylamine and phenobarbital promoted experimental hepatocarcinogenesis.* J Cell Biochem, 2003. **88**(3): p. 578-88.
98. Staruchova, M., et al., *Occupational exposure to mineral fibres. Biomarkers of oxidative damage and antioxidant defence and associations with DNA damage and repair.* Mutagenesis, 2008. **23**(4): p. 249-60.
99. Chen, C., et al., *Increased oxidative damage and mitochondrial abnormalities in the peripheral blood of Huntington's disease patients.* Biochem Biophys Res Commun, 2007. **359**(2): p. 335-40.
100. Duez, P., G. Dehon, and J. Dubois, *Validation of raw data measurements in the comet assay.* Talanta, 2004. **63**(4): p. 879-86.
101. Collins, A.R., et al., *The comet assay: topical issues.* Mutagenesis, 2008. **23**(3): p. 143-51.
102. Krieg, R., et al., *Mitochondrial proteome: cancer-altered metabolism associated with cytochrome c oxidase subunit level variation.* Proteomics, 2004. **4**(9): p. 2789-95.
103. Parrella, P., et al., *Detection of mitochondrial DNA mutations in primary breast cancer and fine-needle aspirates.* Cancer Res, 2001. **61**(20): p. 7623-6.

104. Parrella, P., et al., *Mutations of the D310 mitochondrial mononucleotide repeat in primary tumors and cytological specimens.* Cancer Lett, 2003. **190**(1): p. 73-7.
105. Shen, J., et al., *Mitochondrial copy number and risk of breast cancer: A pilot study.* Mitochondrion, 2009.
106. Ellinger, J., et al., *Mitochondrial DNA in serum of patients with prostate cancer: a predictor of biochemical recurrence after prostatectomy.* BJU Int, 2008. **102**(5): p. 628-32.
107. Moraes, C., *What regulates mitochondrial DNA copy number in animal cells?* Trends Genet, 2001. **17**(4): p. 199-205.
108. Gahan, M., et al., *Quantification of mitochondrial DNA in peripheral blood mononuclear cells and subcutaneous fat using real-time polymerase chain reaction.* J Clin Virol, 2001. **22**(3): p. 241-7.
109. Chen, J., F.F. Kadlubar, and J.Z. Chen, *DNA supercoiling suppresses real-time PCR: a new approach to the quantification of mitochondrial DNA damage and repair.* Nucleic Acids Res, 2007. **35**(4): p. 1377-88.
110. Trevisan, M., et al., *Correlates of markers of oxidative status in the general population.* Am J Epidemiol, 2001. **154**(4): p. 348-56.
111. Fleshner, N.E. and O. Kucuk, *Antioxidant dietary supplements: Rationale and current status as chemopreventive agents for prostate cancer.* Urology, 2001. **57**(4 Suppl 1): p. 90-4.
112. Venkateswaran, V., N.E. Fleshner, and L.H. Klotz, *Synergistic effect of vitamin E and selenium in human prostate cancer cell lines.* Prostate Cancer Prostatic Dis, 2004. **7**(1): p. 54-6.
113. Wu, H.C., et al., *Derivation of androgen-independent human LNCaP prostatic cancer cell sublines: role of bone stromal cells.* Int J Cancer, 1994. **57**(3): p. 406-12.
114. Higuchi, M., et al., *Mitochondrial DNA determines androgen dependence in prostate cancer cell lines.* Oncogene, 2006. **25**(10): p. 1437-45.
115. Pfaffl, M.W., G.W. Horgan, and L. Dempfle, *Relative expression software tool (REST) for group-wise comparison and statistical analysis of relative expression results in real-time PCR.* Nucleic Acids Res, 2002. **30**(9): p. e36.

8. Acknowledgements

I would like to thank my supervisor, Dr. Junjian Z. Chen, for offering me this wonderful opportunity to work in his laboratory and on this project. I am very thankful for vast support he has shown me during all this time.

I would also like to thank my co-supervisor, Dr. Simone Chevalier, for her commentaries and insight on this project.

I would like to thank my thesis advisory committee members: Dr. Anneliese Recklies, Dr. Mario Chevrette and Dr. Terry Chow for their guidance and commentaries.

Additionally, I would like to thank Jinsong Chen and Nadia Passarelli for performing part of the experiments. I would like to thank Phuong-Nam Nguyen and Julie Desautels for proof-reading my thesis.

9. Appendices

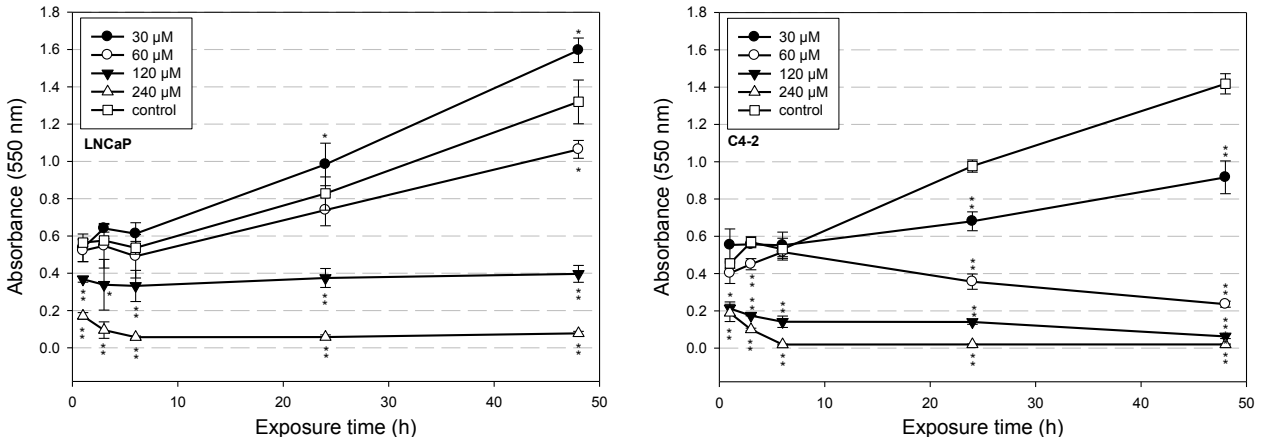

Figure 8 MTT assay with LNCaP and C4-2 prostate cancer cells

MTT assays were performed on LNCaP (A) and C4-2 (B) cells treated to 30 to 240 µM H_2O_2 for 1, 3, 6, 24, and 48 h. The MTT results were calculated from a combination of at least two separate experiments. For each individual experiment, duplicate 96-well plates (12 wells/H_2O_2 treatments) were measured. Statistics were performed by one-way ANOVA with Dunnett's multiple comparison test (* = $p<0.05$, ** = $p<0.01$).

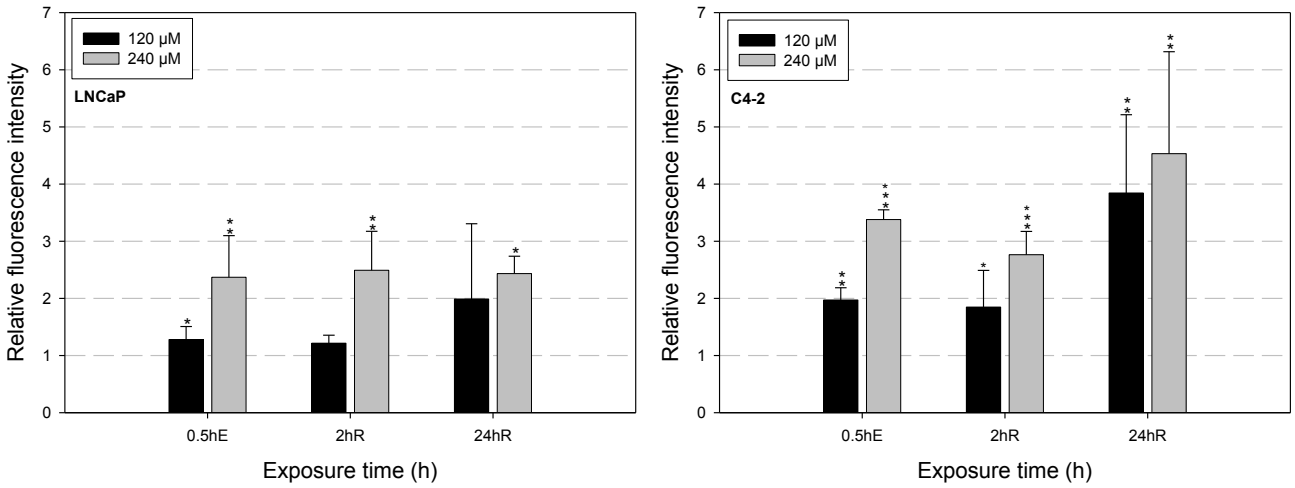

A B

Figure 9 Detection of intracellular production of ROS with fluorescent microscopy
Superoxide was detected and quantified under fluorescent microscopy with DHE. Duplicate dishes of LNCaP (A), and C4-2 (B) cells were treated to 0, 120, and 240 μM H_2O_2 in serum-free medium for 30 min, 30 min with 2 h of recovery, and 30 min with 24 h of recovery. DHE fluorescence was immediately measured after treatment under inverted fluorescent microscopy (IX81, Olympus). All DHE stained images were taken at two random spots on each dish with a TRITC/TR filter, and an exposure time of 25 ms. The relative fluorescence intensity/cell (RFI/cell) data was quantified with Image-Pro 5.0 software (Media Cybernetics) and compared to the untreated control sample (RFI value = 1). The results were calculated from at least two separate experiments. Statistics were performed by one-way ANOVA with Dunnett's multiple comparison test (* = $p<0.05$, ** = $p<0.01$).

Revised Chapter 12

Measuring mtDNA Damage Using a Supercoiling-Sensitive qPCR Approach

Sam W. Chan and Junjian Z. Chen

Abstract

Compromised mitochondrial DNA structural integrity can have functional consequences in mitochondrial gene expression and replication leading to metabolic and degenerative diseases, aging and cancer. Gel electrophoresis coupled with Southern blot and probe hybridization and long PCR are established methods for detecting mtDNA damage. But each has its respective shortcomings: gel electrophoresis is at best semi-quantitative and long PCR does not offer information on the structure. To overcome these limitations, we developed a new method with real-time PCR to accurately quantify the mtDNA structural damage/repair and copy number change. We previously showed that the different mtDNA structures (supercoiled, relaxed circular and linear) have profound influences on the outcome of the real-time PCR amplification. The supercoiled structure is inhibitory to the PCR amplification, while relaxed structures are readily amplified. We will illustrate the use of this new method by quantifying the kinetics of mtDNA damage and repair in LNCaP prostate cancer cells induced by exogenous H_2O_2 treatments. The use of this new method on clinical samples for spontaneous mtDNA damage level will also be highlighted.

Key Words: mtDNA supercoiling, oxidative damage, DNA repair, copy number, real-time PCR.

1. Introduction

Recent studies have shown that alterations in mitochondrial DNA (mtDNA) can induce functional changes that play important roles in metabolic and degenerative diseases, aging and cancer *(1)*. The mitochondrion is responsible for energy production during cellular respiration, and the electron transport chain (ETC) lies at the center of this metabolic function. Situated in the inner membrane, the ETC of the mitochondria supplies energy to the cell through oxidative phosphorylation of ADP to ATP. However, the ETC is

also a major source of reactive oxygen species (ROS) ***(2,3)***. Due to its close proximity and lack of protecting histones, the mtDNA is susceptible to oxidative damage, which can potentially lead to changes in mitochondrial gene expression and somatic mutations in many human cancers ***(4-8)***. In the cells, mtDNA is composed of a mixture of supercoiled, relaxed circular and linear forms. The mature mtDNA has a supercoiled structure with an average of 100 negative super-helical turns ***(9)***. This supercoiled conformation is susceptible to DNA strand breaks induced by oxidative damage, *i.e.*, a single strand break can lead to the disruption of the supercoiled structure. Because the supercoiled conformation is required for initiation of mtDNA replication and transcription *(10-12)*, maintaining the integrity of the mtDNA structure is crucial to normal mitochondria function.

Several techniques have been developed to study mtDNA damage. Gel electrophoresis is frequently used to detect mtDNA conformational changes. However, this assay is not quantitative. It involves a tedious process coupling of Southern blot and probe hybridization. On the other hand, long PCR allows the quantification of mtDNA damage, but it provides little information on the mtDNA structure. To overcome these limitations, we developed a new approach using real-time PCR to quantify structural damage and copy number change of mtDNA. This method is based on several key findings ***(13)***. (a) Supercoiled and relaxed DNA molecules have different efficiencies in PCR amplification. The supercoiled structure inhibits PCR amplification, while relaxed DNA is readily amplified (see **Note 1**). (b) Heat-treatment of DNA templates prior to real-time PCR can be used to artificially introduce strand breaks and relax the mtDNA molecules, allowing quantification of the total amount of mtDNA copies. Thus, this new method is useful for quantifying not only structural damage, repair and copy number change of mtDNA in stressed cells in culture, but also the level of spontaneous damage of mtDNA from clinical samples. In this paper, the new approach will be illustrated by studying mtDNA damage responses to acute oxidative stress in prostate cancer cells (LNCaP) treated by H_2O_2.

2. Materials

2.1 Cell Collection for LNCaP (see Note 2)

1. PBS-CMF, phosphate buffered saline without $CaCl_2$, $MgCl_2$ (GIBCO, Invitrogen cat. No. 20012-027).

2. PBS-CMF/0.5 mM EDTA, to obtain 0.5 mM EDTA, add 500 µl 0.5M EDTA to 500 ml to PBS-CMF; 0.5 M EDTA pH8.0 (GIBCO, Invitrogen cat. No. 15575-020).
3. Trypsin/EDTA solution: 0.05% trypsin + 0.02% EDTA.
4. RPMI media 1640, with L-glutamine.
5. Fetal Bovine Serum (FBS).
6. Penicillin-Streptomycin (10,000 units/ml, 10,000 µg/ml respectively).
7. Complete RPMI medium: remove 50 ml RPMI from 500 ml bottle, add 50 ml FBS (to get 10% FBS) and 5 ml penicillin-streptomycin.
8. Poly-L-lysine (PLL) coated-dish (see **Note 3**).

2.2 DNA Extraction with Genomic-Tip

1. QIAGEN Blood & Cell Culture DNA Kit Mini. The kit contains the following: C1, G2, QBT, QC, QF buffers, protease, 25 genomic tips.

2.2.1. Cell Culture

2. RNase A 2.5 ml (100 mg/ml).
3. Distilled water, DNAse and RNAse free.
4. 1x Tris/EDTA buffer solution (TE buffer): pH 8.0 ± 0.1, 10 mM Tris, and 1 mM EDTA.
5. Isopropanol (2-propanol) for molecular biology grade, minimum 99%.
6. 70% ethanol.

2.2.2. Snap-Frozen Tissue Samples

1. Refer to material in **Section 2.2.1** for cell culture with the following additional material.
2. Proteinase K (>600 mAU/ml).
3. Glass tissue grinder, ground glass Potter-Elvehjem type (Kontes).
4. Sterile surgical scalpel blades and handles.

2.3. DNA Quantification

1. 96-well plate, black opaque, fluorometry compatible.

2.3.1. Fluorometric Quantification of dsDNA Using PicoGreen®

2. Quant-iT™ PicoGreen® dsDNA Assay Kit (Invitrogen, cat. No. P7589). The kit contains PicoGreen dye, 20x TE buffer, and lambda DNA standard (100 µg/ml).
3. Multi-well plate reader with fluorometric capabilities at excitation/emission wavelengths of 480nm/520nm respectively. (PerkinElmer 1420 Multilabel Counter Victor^{3}V).

2.3.2. Quantification by Nanodrop

1. Nanodrop spectrophotometer instrument.
2. Distilled water, DNAse and RNAse free.
3. 1X Tris/EDTA buffer solution (TE buffer): pH 8.0 ± 0.1, 10 mM Tris, and 1mM EDTA.

2.4. Template DNA Preparation and Heat Treatment

1. PCR machine: GeneAmp PCR system 9700 (Applied Biosystems).
2. 1X Tris/EDTA buffer solution, pH 8.0 ± 0.1, 10 mM Tris and 1 mM.

2.5. mtDNA Structural Damage and Repair Analysis Using Real-Time PCR

2.5.1. Bio-Rad System

1. 2X IQ™ SYBR® Green Supermix 500x50 µl reactions (BIO-RAD cat. No. 170-8882).
2. 10 µM primer working solutions (primer sequences listed in **Table 12.1**).
3. Distilled water, DNAse and RNAse free.

Table 12.1
Primer sequences

Gene	Forward primer 5'-3'	Reverse primer 5'-3'
CO2 (mtDNA)	CCCCACATTAGGCTTAAAAACAGAT	TATACCCCCGGTCGTGTAGCGGT
D-loop (mtDNA)	TATCTTTTGGCGGTATGCACTTTTAA CAGT	TGATGAGATTAGTAGTATGGGAGTGG
β-actin	TCACCCACACTGTGCCCATCTACGA	CAGCGGAACCGCTCATTGCCAATGG
β-globin	GTGCACCTGACTCCTGAGGAGA	CCTTGATACCAACCTGCCCAG

4. $MgCl_2$ Solution, 50 mM. (BIO-RAD cat. No. 170-8872).
5. 96-well PCR plates, DNAse and RNase Free (BIO-RAD cat. No. 2239441).
6. Optical tape for plates (BIO-RAD cat. No. 2239444).
7. Real-time PCR detection system: MyIQ™ Single Color Real-Time PCR Detection System with iCycler™ thermocycler base (BIO-RAD).

2.5.2. Applied Biosystems (ABI) System

1. Power SYBR® Fast Green PCR MASTER MIX.
2. 10 μM primer working solutions (primer sequences listed in **Table 12.1**)
3. Distilled water, DNAse and RNAse free.
4. MicroAmp™ Fast Optical 96-well Reaction Plate with Barcode (0.1 ml).
5. Optical tape for plates (ABI).
6. Real-time PCR detection system: 7500 Fast Real-Time PCR System (ABI).

3. Methods

The supercoiled structure of mtDNA is sensitive to experimental artifacts and can be easily disrupted if not properly handled. It is important to always handle the cells and DNA samples with care. The following protocols are designed to minimize potential artificial DNA damage. This section will go through the logical workflow of the experiment from cell collection (**Section 3.1**) → DNA extraction (**Section 3.2**) of cells (**Section 3.2.1**) or frozen tissues (**Section 3.2.2**) → DNA quantification (**Section 3.3**) → template DNA preparation and dilution (**Section 3.4**) → real-time PCR analysis (**Section 3.5**).

LNCaP cells are used as an example for the cell collection protocol. A QIAGEN Blood & Cell Culture DNA Kit is recommended for DNA extraction. Unlike phenol-based methods *(14)* (*see* **Note 4**), this kit employs an ion-exchange system that does not oxidize purines during isolation. The QIAGEN recommended protocol has been modified (*see* **Note 5**) in order to recover both mtDNA and nuclear DNA. The protocol will also apply for frozen tissue preparation (*see* **Note 6**).

Following the DNA extraction, the concentrations of the DNA samples will be quantified. It is recommended (*see* **Note 7**) to perform two rounds of quantifications. The first round will measure the stock concentrations, the second round will measure the precise concentration of 10 ng/μl working solutions prepared from the stock solutions. Two methods are recommended: (**Section 3.3.1**) fluorometric quantification of dsDNA using PicoGreen®, and (**Section 3.3.2**) quantification by Nanodrop® spectrophotometer (*see* **Note 8**).

Prior to the real-time PCR analysis, the half amount of a 1 ng/µl DNA solution will be heat-treated. The original and heated 1 ng/µl DNA templates will be used the detection of the mitochondrial markers (CO2 and/or D-loop) and a 5 ng/µl template for nuclear gene markers (β-actin and β-globin). The method used for real-time PCR analysis is based on the relative quantification model suggested by Pfaffl *(15)*.

3.1. Cell Collection (LNCaP)

1. Remove RPMI medium from the dish by aspiration.
2. Add gently 5 ml PBS-CMF/EDTA, incubate for 1 min at room temperature
3. Remove the PBS-CMF/EDTA and add 2.5 ml of trypsin, incubate for 5 min at 37°C.
4. Resuspend cells by adding 6 ml of RPMI medium to inactivate trypsin; gently aspirate up and down with pipette to get rid of clumps.
5. Transfer cell suspension to a 15 ml tube, and put on ice.
6. Take a small aliquot of cell suspension for cell counting. (should be between 2 to 5 million cells)
7. Centrifuge at ~180 g for 6 min.
8. Remove medium and resuspend cells in 1 ml PBS-CMF. (if the cell suspension has more than 5 million cells, use 2 ml of PBS then split into two 1.5 ml tubes in Step 9)
9. Transfer to 1.5 ml tube, centrifuge at high speed for 2 min.
10. Remove supernatant but not completely, leave just enough to cover the cell pellet. Put on ice.
11. Store at -80°C.

3.2. DNA Extraction with Genomic-Tip for Cell Culture and Snap-Frozen Tissue

This is a modified protocol based on the QIAGEN protocol. Do not use the C1 buffer (*see* **Note 5**). Prewarm the QF buffer to 50°C in a water bath. Cool the 70% ethanol to -20°C.

3.2.1. For Cell Cultures

Prepare protease solution by adding 1.4 ml distilled water to the powdered protease. The recommended amount of cells for each preparation is 2 to 5 million.

1- Thaw cells on ice, resuspend cells by flicking the tube with fingers.

2- Add 1 ml G2 digestion buffer to tube. Immediately vortex at maximum speed for 25 sec (be consistent for all samples). Do

one sample at a time and let the sample rest at room temperature while working with other samples. Centrifuge briefly.

3- Add 3 µl RNase A to each sample. Invert to mix and centrifuge for several seconds.

4- Add 25 µl reconstituted protease. Invert to mix, but do not centrifuge afterwards. Incubate at 50°C for 1h in water bath. Continue on to step 5.

3.2.2. For Snap-Frozen Tissue Samples

Proceed with one sample at a time. It is important to carry out the following steps as fast as possible since the tissue sample can degrade rapidly after thawing. Do not thaw the samples until needed for cutting or grinding (*see* **Note 9**). Homogenize gently manually, any motorized assistance will disrupt the mtDNA structure. It is recommended to carry step 1 to 3 on ice.

1- Prepare a mixture of 1.8 ml G2 buffer + 4µl RNAse A per sample, mix well.

2- Weigh tissue sample (around 10 mg to 50 mg) and cut into smaller piece if needed (see **Note 10**).

3- Add the tissue pieces and ~300 ul of the G2 buffer/RNAse A mixture into a glass tissue grinder to homogenize. Grind manually but do not over-grind as this will disrupt the mtDNA structure (*see* **Note 11**). Collect homogenate into a 2 ml tube. Wash grinder with remaining G2 buffer/RNAse A solution and collect to the 2 ml tube.

4- Add 100 µl proteinase K (see **Note 12**). Invert to mix. Incubate at 50°C for 2 h. Repeat Steps 1-4 for the next sample. Then continue on to Step 5

DNA Extraction with Genomic-tips

5- About 15 min before the end of the incubation at step 4, add 2 ml of QBT buffer to each genomic tip and let the buffer equilibrate the tips.

6- Take the samples out of water bath, and vortex digested samples for 10 s. at maximum speed. Then transfer each sample to a genomic-tip.

7- After the samples have flowed through the tip. Wash the tip with 3 x 1 ml of QC buffer.

8- Elute the DNA into a 15 ml tube by adding 910 ul QF buffer (prewarmed to 50°C) twice into the genomic-tip.

9- Mix the eluted DNA by inverting the tubes and centrifuge at ~188 g. Aliquot solution equally into two 2 ml microcentrifuge tubes (~850 µl).

10- Precipitate the DNA by adding 700-800 µl of isopropanol to each tube. Mix by inverting and incubate for 10 min at room temperature (*see* **Note 13**). Centrifuge at 15,000-18,000 x g for 20 min at 4°C (*see* **Note 14**).

11- Remove and discard supernatant, leaving the DNA pellet at the bottom of the tube. This pellet contains nuclear and mitochondrial DNA.

12- Wash the DNA pellet with 500 µl of 70% ETOH (-20°). Centrifuge at 15000 to 18000 g for 10min at 4°C.

13- Remove and discard the supernatant. Repeat Step 12 once more.

14- Remove the supernatant, three samples at a time, and let the DNA pellet air dry a bit. (*see* **Note 15**)

15- Dissolve DNA pellet with 80-200 µl of TE buffer. Aim for a final concentration of ~ 60 up to ~200 ng/µl.

16- Let the DNA samples sit at 4°C for overnight to ensure that the DNA is completely dissolved.

3.3. DNA Quantification (see Note 7)

3.3.1.Fluorometric Quantification of dsDNA Using PicoGreen ®

3.3.1.1. First Round of Quantification of the Stock DNA Samples

Initial quantification

1- Thaw the PicoGreen® dye in the dark at room temperature.

2- Mix DNA samples by gently flicking the tube. Centrifuge briefly.

3- Prepare the lambda DNA standard. The recommended 2X dilution series range from 20 to 0.625 ng/µl (6 standards).

4- Aliquot 99 µl of TE buffer and 1 µl of DNA sample into a single well. Repeat for duplicate well and go to next sample. It is recommended to first prepare a mix of 198 µl TE buffer and 2 µl DNA in a microcentrifuge tube and then aliquot 100 µl of the mixture into two wells.

5- Aliquot 90 µl TE buffer and 10 µl of the lambda standard into a well. Repeat for duplicate well and go to next lambda standard.

6- Prepare PicoGreen® solution: aliquot 5 µl of stock PicoGreen® into 0.995 ml TE buffer; 100 µl of this mixture is required for each well (keep in dark).

7- Aliquot 100 µl of PicoGreen® solution into each well, then mix by pipetting up and down.

8- Incubate in the dark at room temperature for 10min.

9- Perform fluorometric measurement using a multiplate reader at excitation/emission lengths of 480 nm/520 nm.

10- Calculate the concentration of the stock DNA samples from the standard curve.

11- Prepare a 10 ng/µl working solution from each stock DNA sample (volume: around 200 µl).

3.3.1.2. Second Round of Quantification of the 10 ng/µl DNA Samples

Precise quantification

1- Repeat the steps from "First Round of Quantification". Add 90 µl TE buffer and 10 µl 10 ng/µl of DNA sample into each well this time.

2- Measure the concentration of 10 ng/µl DNA working solutions. 1 and 5 ng/µl DNA templates will be prepared from each working solution.

3.3.2. Quantification by Nanodrop® (For model ND-1000) (see Note 8)

1. Choose the nucleic acid assay option from the Nanodrop software.
2. Initialize the machine with distilled water. Pipette 1 µl of water onto reading pedestal. Click OK.
3. Wipe off water with clean tissue; make a blank reading with 1 µl TE buffer. Click Blank.
4. Place 1 µl of DNA sample and click measure. After each reading, wipe off with clean tissue.
5. Take triplicate measurements of each sample and use the average of the results.
6. Prepare 10 ng/µl working solutions from stocks. Quantify again to get precise measurements.

3.4. Template DNA Preparation and Heat Treatment

1- Prepare 5 ng/µl templates in TE buffer from the 10 ng/µl working solutions. (Volume: 200 µl)

2- Prepare 1 ng/µl templates in TE buffer from the 5 ng/µl templates. (Volume: 100 µl)

3- Aliquot 50 µl of 1 ng/µl DNA into a PCR tube And proceed with heat-treatment in Step 4. The remaining half will serve as the original template.

4- Perform heat treatment on 50 µl of 1 ng/µl DNA by following this PCR protocol: 95°C for 6min and 10°C for cool down.

5- 5 ng/µl DNA will be used for quantifying nuclear markers, and 1 ng/µl original and heated DNA will be used for mitochondrial markers.

6- Prepare a five-point standard using the stock DNA of the control sample. The recommended standard is a 5X dilution series ranging from 40 to 0.064 ng/µl. (*see* **Note 16**)

3.5. mtDNA Structural Damage and Repair Analysis Using Real-Time PCR

To ensure optimal reproducibility, always prepare a master mix containing the SYBR Green Supermix and primers, and use aliquots of this mixture with individual DNA samples. As an example, LNCaP cells are treated with exogenous H_2O_2 to measure mtDNA damage during exposure and repair activity during recovery (**Fig. 12.1**). The following protocol is performed in 30 µl reaction in triplicate using the Bio-Rad system.

1- Mix samples and standards gently by flicking. Centrifuge briefly.

2- Prepare and label 0.5 ml tubes for each sample and standard.

3- Prepare the total amount of master mix needed by adding the reagents in this specific order (**Table 12.2**), based on a six paired samples (*i.e.*, for six each original and heated 1 ng/µl DNA) and five standards.

Table 12.2
(*see* Note 17)

Template points (triplicate, 30 µl/well)	Reactions	Reagents	1X	54X
5 DNA standards	15X	Distilled H_2O	10.8 µl	583.2 µl
6 Original 1 ng/µl DNA	18X	50 mM $MgCl_2$	0.6 µl	32.4 µl
6 Heated 1 ng/µl DNA	18X →	10 µM Forward primer	0.9 µl	48.6 µl
1 Blank	3X	10 µM Reverse primer	0.9 µl	48.6 µl
	54X	2X SYBR Mix (Bio-Rad)	15 µl	810 µl
			28.2 µl	1,522.8 µl

4- Aliquot 5.4 µl of DNA template into a 0.5 ml tube, add 84.6 µl of the master mix. Mix well by pipetting up and down. Put tube on ice until ready to load into wells.

5- Repeat Step 4 for each sample and standard.

6- Aliquot each template mixture into three wells (30 µl per well). Be careful to deposit the aliquot at the bottom of the well without creating bubbles. Avoid cross-contamination of the wells. Blank solutions without DNA will serve as negatives.

7- Seal the plate with optical tape. If necessary, centrifuge the plate briefly to get rid of bubbles.

8- PCR program for mtDNA markers on the Bio-Rad system: cycle 1 (1X), 95.0°C for 1.5 min; cycle 2 (30X), step 1 at 95.0°C for 20 sec, step 2 at 61.0°C for 30 sec; cycle 3 (1X), 95.0°C for 1 min; cycle 4 (1X), 55.0°C for 1 min, cycle 5 (40X) 55.0°C for 10 sec with an increase of 1.0°C after each repeat for collecting melt curve data. Enable real-time data collection at cycle 2 step 2 (for ABI system, *see* **Note 18**).

9- At least one nuclear DNA marker is analyzed to serve as a reference gene for the analysis. To run nuclear gene, calculate the amount of each reagent based on triplicates of five standards, six 5 ng/µl DNA samples, and one blank (36X). The PCR program is the same as in Step 8, except for 40X at cycle 2 (for ABI system, *see* **Note 19**).

10- The data can be analyzed with any relative expression software tool (REST) which is based on the Pfaffl formula:

$$R = \frac{\left(Efficiency_{target\ gene}\right)^{\Delta CP\ target(Mean\ Control - Mean\ sample)}}{\left(Efficiency_{reference\ gene}\right)^{\Delta CP\ ref(Mean\ Control - Mean\ sample)}}$$

Assign a nuclear gene as the reference gene and use the original 1 ng/µl from the control sample as the calibrator for analysis. (**Fig. 12.2**) (*see* **Note 20**)

4. Notes

1. The supercoiled structure inhibits the binding of oligonucleotide primers, preventing further amplification. In contrast, the relaxed forms (open circular and linear) allow effective primer binding and subsequent DNA polymerization. Thus, the relaxed forms of mtDNA are better substrates for PCR than supercoiled mtDNA.
2. Listed materials for prostate cancer LNCaP cells. Substitute with appropriate reagents and buffers for cell lines to be used.

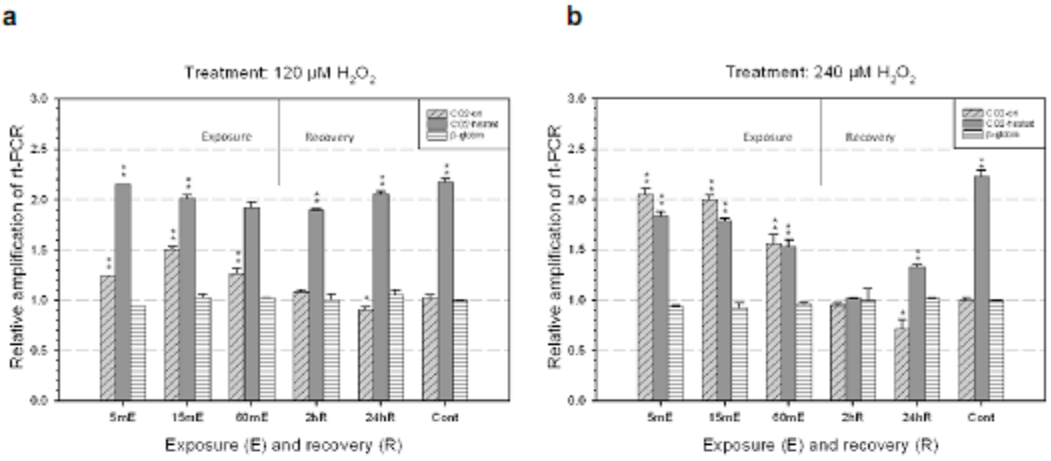

Fig. 12.1. **MtDNA damage responses to oxidative damage in LNCaP prostate cancer cells induced by exogenous H_2O_2 treatment.** Two concentrations (120 μM and 240 μM) of H_2O_2 were used to induce oxidative stress in LNCaP cells. For exposure, LNCaP cells were treated for 5, 15 and 60 min to induce DNA damage. For recovery, LNCaP cells were first treated for 60 min, and then allowed to recover in fresh medium for 2 and 24 h. The CO2 mitochondrial marker was normalized with the nuclear marker β-actin; a second nuclear marker β-globin was shown to indicate the lack of structural change in the target nuclear genes. The diagonally striped bars represent the relaxed mtDNA fraction in the original DNA template. The solid gray bars represent the total mtDNA content in the pre-heated mtDNA template. Changes in relaxed mtDNA fraction and total mtDNA content correspond to mtDNA damage and copy number change, respectively, in treated samples. (A) At low concentration of H_2O_2 (120 μM), LNCaP cells showed early increase of mtDNA structural damage from 5 minE to 60 minE when compared to control, but the damage was repaired 24 h after the treatment. The total mtDNA content remained stable. (B) While at a higher concentration of H_2O_2 (240 μM), LNCaP showed acute early mtDNA structural damage, reflecting complete disruption of mtDNA structure in the original template. The damage was not repaired 24 h after the treatment, resulting in a significant loss of mtDNA content as indicated by decreases of total mtDNA signals in pre-heated templates. Statistics performed by one-way ANOVA, compared to original fraction of control (* = $p<0.05$, ** = $p<0.01$). (*see* **Note 21**)

3. LNCaP cells detach easily in regular culture dishes. Prepare PLL coated dishes by adding 3 ml of 1% PLL solution to a 100 mm dish. Incubate for 5 min, then remove all solution from the dish. Dry in fume hood overnight.
4. There are other methods for DNA extraction such as Trizol. It is shown that the Trizol procedure disrupts most structural features from the mtDNA (data not shown).
5. The C1 step removes cellular organelles including mitochondria during preparation, leadin to loss of mtDNA.
6. Fresh snap-frozen tissue samples are suitable for structural analysis, but not paraffin-embedded tissues due to crosslinking.

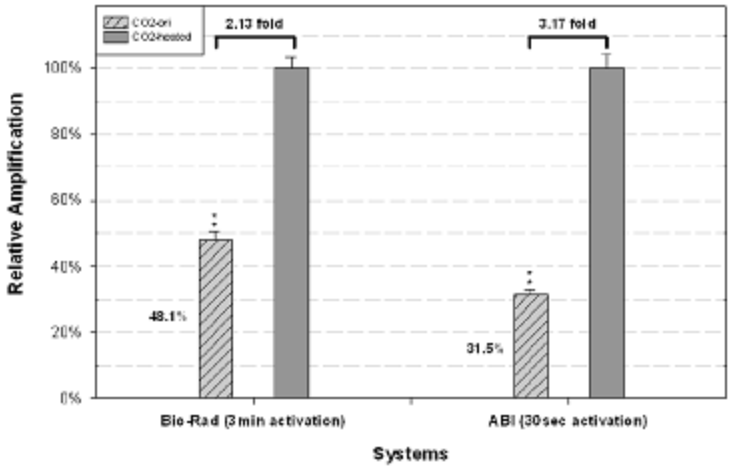

Fig 12.2. **Baseline levels of mtDNA damage in non-treated prostate cancer cells analyzed by two qPCR systems: Bio-Rad *vs.* ABI.** The baseline level of damage and the spontaneous damage are two distinct features. The baseline level of damage is the amount of mtDNA damage that is being detected by the systems. Artifacts introduced during the sample preparation and the initial heat-activation of real-time PCR can increase the baseline level of damage. On the other hand, spontaneous damage represents the actual amount of endogenous mtDNA damage of non-treated samples. The mtDNA structure is heat sensitive, and consequently the initial enzyme activation step at 95°C required by the real-time PCR protocol can potentially introduce artificial damage to the mtDNA structure. By shortening this step, it is possible to reduce this artificial damage. This figure compares the relative amplification of non-treated C4-2 (an isogenic variant of LNCaP) DNA using Bio-Rad and ABI systems at 3 min and 30 sec of initial 95°C activation, respectively. The Bio-Rad system detected 48.1% of damaged mtDNA, while the ABI system detected 31.5% of damage. A reduction of 34.5% was observed between the two systems, representing the removal of substantial amount of artificial damage by the ABI system. As such the baseline level of damage detected with the ABI system is more representative of the spontaneous level of mtDNA damage. The differences observed between the two systems can be attributed to the shorter initial heat-activation time as well as the different enzyme chemistry used. Statistics were performed with t-test, the two groups were found significantly different (Bio-Rad (3 min), n=4; ABI (30 sec), n=3; ** = $p<0.01$) (*see* **Note 22**)

7. The 2-step DNA quantification is optional but recommended. Since this will limit the dynamic range of the samples during real-time PCR amplification, leading to reproducible quantification.
8. A conventional spectrophotometer can also be used for the two-step DNA quantification. We recommend using the Nanodrop spectrophotometer which requires only 1-2 μl of DNA sample for precise measurement.
9. It is not recommended to repeatedly freeze and thaw the same samples as this can degrade the quality of the DNA. If the tissue sample is to be used on separate occasions, cut the tissue into to smaller pieces and thaw only what is needed.

10. Work fast. It is not recommended to thaw the tissue sample until it is ready to be homogenized in the glass homogenizer. If the tissue sample is too hard to cut, thaw on wet ice.
11. After homogenization, there will still be residue pieces of tissue that are not completely homogenated. Don't continue grinding because this will disrupt the DNA structure. Transfer everything to a 2 ml tube. Proteinase K will digest the remaining pieces.
12. Proteinase K is used instead of the protease included in the kit because the former is more efficient in digesting the remaining tissue in the homogenate.
13. Unless the sample is exposed to harsh treatments during experiments, the precipitated DNA should look like long intertwined DNA fibers.
14. The DNA fiber is mostly nuclear DNA; mtDNA is too small to be seen in suspension. The high-speed centrifugation is needed to bring down the mtDNA and to form a pellet with nuclear DNA.
15. Do not over-dry as this will make it harder to dissolve in TE buffer.
16. A standard is needed to take into consideration of PCR efficiency when using Pfaffl's relative quantification model. The standard is not required for the $\Delta\Delta$Ct method, but the efficiencies of different markers have to be optimized and validated.
17. It is recommended to add an additional 3-4 µl of distilled water to the final mixture to compensate for the loss due to pipetting.
18. PCR program for mtDNA markers on the ABI system: cycle 1 (1X), 95.0°C for 30sec; cycle 2 (30X), step 1 at 95.0°C for 3sec, step 2 at 61.0°C for 30sec; cycle 3 (1X) add melt curve. Enable real-time data collection at cycle 2 step 2.
19. PCR program for nuclear DNA on the ABI system: cycle 1 (1X), 95.0°C for 30 sec; cycle 2 (40X), step 1 at 95.0°C for 3 sec, step 2 at 61.0°C for 30 sec; cycle 3 (1X) add melt curve. Enable real-time data collection at cycle 2 step 2.
20. There are various REST tools that are freely available on the internet: REST-XL, REST-MCS, and others.
21. Similar results were obtained by analyzing with the D-loop mitochondrial marker.
22. Similar results were observed with other cell lines, frozen tissues, and blood leukocyte samples. The Power SYBR® Fast Green PCR MASTER MIX from ABI and its 7500 Fast Real-Time

PCR System platform made it possible to cut down the initial 95°C activation time to 30sec (*see* **Note 18**). This should be taken into consideration when analyzing clinical samples where small differences in spontaneous damage levels need to be measured.

References

1. Wallace, D.C. (2005) A mitochondrial paradigm of metabolic and degenerative diseases, aging, and cancer: a dawn for evolutionary medicine. *Annu. Rev. Genet.*, **39**, 359 407.
2. Turrens,J.F. and Boveris,A. (1980) Generation of superoxide anion by the NADH dehydrogenase of bovine heart mitochondria. *Biochem. J.*, **191**, 421-427
3. Richter,C. (1995) Oxidative damage to mitochondrial DNA and its relationship to ageing. *Int. J. Biochem. Cell Biol.*, **27**, 647-653
4. Toyokuni S, Okamoto K, Yodoi J, Hiai H. (1995) Persistent oxidative stress in cancer. *FEBS Lett.* **358**, 1–3.
5. Herrmann PC, Gillespie JW, Charboneau L, Bichsel VE, Paweletz CP, Calvert VS, Kohn EC, Emmert-Buck MR, Liotta LA, et al. (2003) Mitochondrial proteome: altered cytochrome c oxidase subunit levels in prostate cancer. *Proteomics*. **3**,1801–1810.
6. Fliss MS, Usadel H, Caballero OL, Wu L, Buta MR, Eleff SM, Jen J, Sidransky D. (2000) Facile detection of mitochondrial DNA mutations in tumors and bodily fluids. *Science*. **287,** 2017–2019.
7. Parrella P, Xiao Y, Fliss M, Sanchez-Cespedes M, Mazzarelli P, Rinaldi M, Nicol T, Gabrielson E, Cuomo C, et al. (2001) Detection of mitochondrial DNA mutations in primary breast cancer and fine-needle aspirates. *Cancer Res*. **61,** 7623–7626.
8. Chen JZ, Gokden N, Greene GF, Mukunyadzi P, Kadlubar FF. (2002) Extensive somatic mitochondrial mutations in primary prostate cancer using laser capture microdissection. *Cancer Res*. **62**, 6470–6474.
9. Radloff,R., Bauer,W. and Vinograd,J. (1967) A dye-buoyant-density method for the detection and isolation of closed circular duplex DNA: the closed circular DNA in HeLa cells. *Proc. Natl. Acad. Sci. USA*, **57**, 1514-1521
10. Robberson, D.L. and Clayton, D.A. (1972) Replication of mitochondrial DNA in mouse L cells and their thymidine kinase-derivatives: displacement replication on a covalently-closed circular template. *Proc. Natl. Acad. Sci USA*, **69**, 3810-3814
11. Bogenhagen,D. and Clayton, D.A. (1978) Mechanism of mitochondrial DNA replication in moouse L-cells: introduction of superhelical turns into newly replicated molecules. *J. Mol. Biol.*, **119**, 69-81
12. Clayton, D.A. (1982) Replication of animal mitochondrial DNA. *Cell*, **28**, 693-705
13. Chen,J., Kadlubar F.F., and Chen J.Z., (2007) DNA supercoiling suppresses real-time PCR: a new approach to the quantification of mitochondrial DNA damage and repair. Nucleic Acids Research, **35**(4), 1377-1388
14. Ayala-Torres,S., Chen,Y., Svoboda,T., Rosenblatt,J. and Van Houten,B. (2000) Analysis of gene-specific DNA damage and repair using quantitative polymerase chain reaction. *Methods*, **22**, 135-147.
15. Pfaffl M. W. (2001) A new mathematical model for relative quantification for real-time RT-PCR. *Nucleic Acid Research*, **29**, 9 00